

Molecular dynamics description of an expanding q/\bar{q} plasma with the Nambu–Jona-Lasinio model and applications to heavy ion collisions at RHIC and LHC energies

R. Marty^{1,2,3,*} and J. Aichelin¹

¹*Subatech (UMR 6457, IN2P3/CNRS), Université de Nantes, École des Mines de Nantes, 4 rue Alfred Kastler, 44307 Nantes cedex 3, France*

²*Frankfurt Institut for Advanced Studies, Johann Wolfgang Goethe Universität, Ruth-Moufang-Str. 1, 60438 Frankfurt am Main, Germany*

³*Institut for Theoretical Physics, Johann Wolfgang Goethe Universität, Max-von-Laue-Str. 1, 60438 Frankfurt am Main, Germany*

We present a relativistic molecular dynamics approach based on the Nambu–Jona-Lasinio Lagrangian. We derive the relativistic time evolution equations for an expanding plasma, discuss the hadronization cross section and how they act in such a scenario. We present in detail how one can transform the time evolution equation to a simulation program and apply this program to study the expansion of a plasma created in experiments at RHIC and LHC. We present first results on the centrality dependence of v_2 and of the transverse momentum spectra of pions and kaons and discuss in detail the hadronisation mechanism.

PACS numbers: 24.10Cn, 24.10Jv, 24.85+p

Keywords: molecular dynamics, relativistic dynamics, constrained hamiltonian, Quark-Gluon-Plasma, Nambu–Jona-Lasinio model, hadronization, collective phenomena

I. INTRODUCTION

The interpretation of the results of ultrarelativistic heavy ion collisions is presently one of the most challenging problems in theoretical nuclear physics. In these collisions, investigated at the Relativistic Heavy Ion Collider (RHIC) at the Brookhaven National Laboratory and at the Large Hadron Collider (LHC) at CERN, more than thousand particles are observed in central collisions. Although the multiplicity and the single particle transverse momentum spectra at midrapidity of the different particle species are of interest by their own right, the purpose of the experiments is to find out whether during the reaction the matter has made a transition towards a new state of matter, a Quark-Gluon Plasma (QGP). This information is not directly visible in the measured hadron spectra and therefore theoretical approaches have to be employed to verify whether the measured observables are compatible with the existence of such a QGP or, even more wanted, whether they can even lead to the conclusion that such a state is necessary to explain the measured quantities.

The state of the art theoretical approaches aim at a complete description of the heavy ion reaction, from the initial separation of projectile and target up to the momenta of the finally observed particles [1, 2]. Almost all of the presently developed models assume that quite early in the heavy ion reaction a QGP in local equilibrium is established and that hence the further evolution of the system can be described by the hydrodynamical equations before finally hadronisation takes place. Employing the

equation of state, calculated by lattice gauge calculations, taking into account initial state fluctuations and assuming that the Cooper-Frye formalism describes hadronisation correctly, these models have been quite successful in describing many of the observables.

To bridge the yet unknown physics these models necessarily rely on a number of assumptions which are highly debated. They assume that very early during the interaction a local equilibrium is established which is hard to understand in view of the magnitude of perturbative Quantum Chromo Dynamics (pQCD) cross sections. How this can happen is therefore not clear yet. They also assume that no correlations among plasma constituents are built up during the expansion and that therefore the hadron production is just determined by temperature, chemical potential and the collective velocity of the fluid cell at the moment of hadronization which is considered as *instantaneously*.

Therefore it may well be that these hydrodynamical models don't contain the correct physics. As an example for the ambiguity of the theoretical interpretation of experimental results we just mention the centrality dependence of the elliptical flow, one of the key observables, which is equally well reproduced in three quite different approaches. In approaches which use *viscous* hydrodynamics [3] this centrality dependence serves to determine the viscosity of the QGP and therefore of the interaction among the constituents of the plasma, the quarks and the gluons. In *ideal* hydrodynamical approaches with fluctuating initial conditions [2, 4], in which only regions of a high energy density form a QGP, this centrality dependence is due to the impact parameter dependence of the relative contributions of high energy density and of low energy density regions. Finally, the centrality dependence is also well described in the core-corona model [4]

*Email : marty@fias.uni-frankfurt.de

which assumes that nucleons which suffer from only one hard initial scattering fragment like a proton in p-p collisions whereas the rest forms a QGP whose properties are impact parameter independent.

Due to these facts it is worthwhile to test the assumptions on which the application of hydrodynamical models is based. In order to do this one needs models which do not assume right from the beginning that a local equilibrium is established. The Parton Hadron String Dynamics (PHSD) [5–7] is such a model which allows to study the plasma evolution by solving a Boltzmann type equation. There potentials between the plasma constituents are chosen in such a way that the equation of state from lattice calculations is respected. Cross sections can be derived from the space like part of the interaction and are employed for the scattering interactions among the plasma constituents. In this model gluons as well as quarks acquire a large mass when approaching the phase transition. Therefore the prehadrons which are created at the phase transition are rather heavy. Pions and other light hadrons are produced by the decay of these prehadrons. Another model which allows for these studies is a gluonic cascades realized in the Boltzmann Approach to Multi Parton Scattering (BAMPS) [8]. The gluon emissions and interactions during the expansion of the QGP move the system toward equilibrium.

A while ago a third approach has been advanced [9] which is based on the Nambu–Jona-Lasinio (NJL) Lagrangian [10, 11]. This Lagrangian is an approximation to the QCD Lagrangian which respects all its symmetries. In the version which includes a Polyakov loop (PNJL) this approach also describes the equation of state of the lattice QCD data [12]. It has the advantage that all free parameters of the Lagrangian can be determined by static meson properties, like meson masses and decay constants. It contains no explicit gluons assuming that the in-medium mass of the gluons is large as compared to the transferred momentum and therefore the interaction of the quarks is effectively a contact interaction. The quarks interact by scalar fields and by cross sections which can be as well derived from the Lagrangian [13, 14]. Mesons can be produced, even in the deconfined phase, but they are unstable there and may decay. Only when the system approaches the cross over (for low chemical potential the (P)NJL Lagrangian shows a cross over and not a phase transition) the finite width of the meson mass disappears and stable mesons can emerge from the system. The light mesons are directly produced by $q\bar{q}$ scattering. Similar to the PHSD approach this Lagrangian offers therefore the opportunity to study the evolution of the system from the creation of a plasma up to the finally observed mesons. Using a N-body molecular dynamics approach it is possible to study correlations and fluctuations which are built up during the expansion phase and to investigate whether observables can be identified which are sensitive to them.

The cross sections calculated in this approach are quite small deep inside the plasma phase but, due to s channel

resonances, they are quite large close to the cross over [14] where the system behaves like a liquid. Deep in the plasma phase the particles have only their bare mass and move with a velocity which is close to the velocity of light. In order to study the time evolution of the N-body system with the NJL Lagrangian we have therefore to develop a molecular dynamics approach for interacting particles which move relativistically. Such an approach was advanced in the original paper of the Relativistic Quantum Molecular Dynamics (RQMD) [15] approach but has never been used in practice because of conceptual and of numerical problems. Some of the conceptual problems are related to the choice of constraints which one has to impose to construct such a relativistic molecular dynamics.

The papers which contain the mathematical tools to develop a relativistic molecular dynamics approach are widely scattered. Therefore, and in order to present a comprehensive approach, we will start out in the next section with a presentation of the formalism and its derivation. We will describe how a relativistic molecular dynamics can be developed, how one can avoid the No Interaction Theorem (NIT) and how the Dirac approach for Hamiltonian system with constraints is of importance for the development of a relativistic dynamics. Finally we present the formalism which is used. We discuss the constraints and their consequences for the dynamics. The third section presents the NJL model as far as it is necessary to understand our approach, in particular we discuss how masses and cross sections can be calculated. The fourth section is devoted to the details of the numerical realization of the approach. In the fifth section we present how we validated the program and some results. Finally, in the sixth section, we draw our conclusions.

II. RELATIVISTIC QUANTUM MOLECULAR DYNAMICS

A. Molecular Dynamics

1. 1-body Classical Molecular Dynamics

In the classical molecular dynamics approach particles are moving under the mutual influence of forces. The goal is to describe the trajectories of these particles in phase space $(\mathbf{q}_i(t), \mathbf{p}_i(t))$. Knowing the phase space point for a given initial condition $(\mathbf{q}_i(0), \mathbf{p}_i(0))$ and the Hamiltonian \mathcal{H} we can predict the phase space points at any given moment t and can calculate the value of each observable which is defined on the classical phase space. The trajectory may depend in a very sensible way on the initial condition and may therefore become chaotic. Such systems are, however, not of interest here.

We start the discussion by providing the formalism. We employ the Hamilton-Jacobi approach to formulate the motion of one particle in phase space. The equation of motion for an observable A , defined on the classical

phase space, $A(\mathbf{q}, \mathbf{p}, t)$, where $\mathbf{q}, \mathbf{p}, t$ are the independent variables, is given by

$$\frac{d}{dt}A(\mathbf{q}, \mathbf{p}, t) = \frac{\partial A}{\partial t} + \frac{\partial A}{\partial \mathbf{q}} \frac{\partial \mathbf{q}}{\partial t} + \frac{\partial A}{\partial \mathbf{p}} \frac{\partial \mathbf{p}}{\partial t}. \quad (1)$$

The Hamilton-Jacobi equations, which present the equations of motion of the phase space coordinates \mathbf{q} and \mathbf{p} in time can be obtained by a variational principle

$$\begin{aligned} \frac{d\mathbf{q}}{dt} &= \frac{\partial \mathcal{H}}{\partial \mathbf{p}} \\ \frac{d\mathbf{p}}{dt} &= -\frac{\partial \mathcal{H}}{\partial \mathbf{q}}, \end{aligned} \quad (2)$$

where $\mathcal{H}(\mathbf{q}, \mathbf{p})$ is the Hamiltonian of the system. We can bring eq. (1) into the form

$$\frac{dA}{dt} = \frac{\partial A}{\partial t} + \{A, \mathcal{H}\}. \quad (3)$$

$\{A, B\}$ is the Poisson's bracket of A and B defined for N particles as

$$\{A, B\} = \sum_k^N \frac{\partial A}{\partial \mathbf{q}_k} \frac{\partial B}{\partial \mathbf{p}_k} - \frac{\partial A}{\partial \mathbf{p}_k} \frac{\partial B}{\partial \mathbf{q}_k}. \quad (4)$$

In the special case where A does not explicitly depend on time we find

$$\frac{dA}{dt} = \{A, \mathcal{H}\}. \quad (5)$$

If we replace A by either \mathbf{q} or \mathbf{p} we recover the Hamilton-Jacobi equations, eq. (2)

$$\begin{aligned} \frac{d\mathbf{q}}{dt} &= \{\mathbf{q}, \mathcal{H}\} = \frac{\partial \mathcal{H}}{\partial \mathbf{p}} \\ \frac{d\mathbf{p}}{dt} &= \{\mathbf{p}, \mathcal{H}\} = -\frac{\partial \mathcal{H}}{\partial \mathbf{q}}. \end{aligned} \quad (6)$$

For a given initial condition $(\mathbf{q}_0, \mathbf{p}_0)$ these equations can be solved, analytically or at least numerically, and we obtain the desired trajectory of the particle in phase space. For the later discussion it is important to note that eqs. (6) are the differential equation for the trajectory on which the energy \mathcal{H} is conserved.

2. *N-body (Quantum) Molecular Dynamics*

This approach can be easily extended towards several mutually interacting particles and also towards Quantum Mechanics. The starting point for finding the time evolution of a classical N -body system is the N -body Hamiltonian

$$\mathcal{H} = \sum_i^N \frac{\mathbf{p}_i^2}{2m} + \sum_{i \neq j}^N V(\mathbf{q}_i, \mathbf{p}_i, \mathbf{q}_j, \mathbf{p}_j) \quad (7)$$

where $V(\mathbf{q}_i, \mathbf{p}_i, \mathbf{q}_j, \mathbf{p}_j)$ is the two body potential between particle i and j . For a given initial conditions $(\mathbf{q}_i(t=0), \mathbf{p}_i(t=0))$ the Hamilton-Jacobi equations (2) can be solved analytically or numerically. This approach has been extended in the eighties toward the Quantum Molecular Dynamics (QMD) approach, a theory which has been successfully applied to simulate heavy ion reactions in the energy range between $50 \text{ AMeV} \leq E_{kin} \leq 2 \text{ AGeV}$ [16]. This approach allowed to clarify the origin of multifragmentation [17], the production of mesons close to threshold [18] and the equation of state of hadronic matter [19] well above normal nuclear matter density. It is based on a time dependent version of the Ritz variational principle and starts out from a trial wave function of a Gaussian form. The Wigner density of this trial wave function is defined on the phase space and has the form

$$f(\mathbf{q}_i, \mathbf{p}_i, t) \propto \exp \left(-\frac{(\mathbf{q}_i - \mathbf{q}_i^0(t))^2}{L} \right) \cdot \exp \left(-(\mathbf{p}_i - \mathbf{p}_i^0(t))^2 L \right). \quad (8)$$

Assuming now that the wave function of the N -body system is a product of the single particle wave functions and that the centroids $\mathbf{q}_i^0(t), \mathbf{p}_i^0(t)$ of the Gaussians depend on time whereas the width is constant, the variational principle gives the following equations of motion

$$\begin{aligned} \frac{d\mathbf{q}_i^0}{dt} &= \frac{\partial \langle \mathcal{H} \rangle}{\partial \mathbf{p}_i^0} \\ \frac{d\mathbf{p}_i^0}{dt} &= -\frac{\partial \langle \mathcal{H} \rangle}{\partial \mathbf{q}_i^0}, \end{aligned} \quad (9)$$

with $\langle \mathcal{H} \rangle$ being the expectation value of the Hamiltonian with respect to the trial wave function. For details we refer to [16].

B. Relativistic phase space and transformations between inertial systems

1. Minkowski phase space

One may have the idea that the equations of motion for relativistic particles can be obtained by replacing in eq. (6) the three dimensional vectors \mathbf{r} and \mathbf{p} by four dimensional vectors q^μ and p^μ . This is, however, not true:

- replacing in eq. (2) \mathbf{q} by q^μ and \mathbf{p} by p^μ one finds an equation which is not covariant because \mathcal{H} is the zero component of the energy-momentum 4-vector.
- eq. (2) contains a derivative with respect to the time t . In a relativistic theory the time is just the zero component of the space-time 4-vector. For N particles we have furthermore N different times and it is not evident how these times are related to variable t of eq. (2).

c) these equations describe the motion of particles in an 8 dimensional phase space in which neither the energy is conserved nor the times of the different particles are synchronized. In a molecular dynamics approach we are interested to obtain physical trajectories in a $6N + 1$ dimensional phase space $(\mathbf{q}_i(\tau), \mathbf{p}_i(\tau))$, i.e. world lines of the particles, and we want to know at which position in coordinate and momentum space the particle is located for a given value of the time evolution parameter τ (whose nature will be discussed later).

Thus a Hamiltonian in a nonrelativistic sense (the total energy of the system) has no place in a relativistic approach. If we talk later of an "Hamiltonian" in relativistic dynamics and of time evolution equations which have a form similar to eq. (2) the meaning of the different terms in this equation will be completely different as compared to that in a non-relativistic theory.

We start out from the 4-position and 4-momentum coordinates (q_k^μ, p_k^μ) as *canonical* variables which obey

$$\begin{aligned} \{q_a^\mu, q_b^\nu\} &= \{p_a^\mu, p_b^\nu\} = 0 \\ \{q_a^\mu, p_b^\nu\} &= \delta_{ab} g^{\mu\nu} \end{aligned} \quad (10)$$

with $g^{\mu\nu}$ being the Minkowski metric with the diagonal $\{1, -1, -1, -1\}$ and zero otherwise. Here we have introduced the Poisson brackets for 4-vectors

$$\{A, B\} = \sum_{k=1}^N \frac{\partial A}{\partial q_k^\mu} \frac{\partial B}{\partial p_{k\mu}} - \frac{\partial A}{\partial p_k^\mu} \frac{\partial B}{\partial q_{k\mu}}. \quad (11)$$

Because in a dynamical system q^μ and p^μ depend on the time evolution parameters τ , these quantities have to be taken at equal τ .

2. Poincaré Group and Algebra

Relativistic theories have to be invariant under Lorentz transformations Λ and space-time translations a . Both transformations form the Poincare group with the group element $R(\Lambda, a)$. It consists of all transformations of the form

$$q'^\mu = R(\Lambda, a) q^\mu = \Lambda_\nu^\mu q^\nu + a^\mu \quad (12)$$

which leave the scalar product between two 4-vectors unchanged

$$q'_\mu q'^\mu = q_\mu q^\mu \quad (13)$$

with $q^\mu = (t, \mathbf{q})$ and $q_\mu = g_{\mu\nu} q^\nu$.

The algebra associated with the continuous symmetry group is given by the algebra of the generators of infinitesimal transformations. Finite transformations can be built with help of the infinitesimal ones. We start out with a Lorentz transformation which differs only infinitesimally from the neutral element $R(\mathbb{1}, 0)$

$$\Lambda_\nu^\mu = \mathbb{1} + \Delta\omega_\nu^\mu \quad (14)$$

with $\Delta\omega$ being small. The invariance of the scalar product of 4-vectors under a Lorentz transformation can be expressed as

$$\begin{aligned} q'_\mu q'^\mu &= q'^\mu g_{\mu\nu} q'^\nu = \Lambda_\sigma^\mu q^\sigma g_{\mu\nu} \Lambda_\rho^\nu q^\rho \\ &= q^\mu g_{\mu\nu} q^\nu = q_\mu q^\mu \end{aligned} \quad (15)$$

and hence

$$\begin{aligned} g_{\sigma\rho} &= \Lambda_\sigma^\mu g_{\mu\nu} \Lambda_\rho^\nu \\ &= g_{\mu\nu} (\delta_\sigma^\mu + \Delta\omega_\sigma^\mu) (\delta_\rho^\nu + \Delta\omega_\rho^\nu) \\ &= g_{\sigma\rho} + \Delta\omega_{\sigma\rho} + \Delta\omega_{\rho\sigma} + \mathcal{O}(\Delta\omega^2). \end{aligned} \quad (16)$$

Consequently $\Delta\omega_{\mu\nu}$ has to be antisymmetric. There are 6 independent elements which satisfy

$$\Delta\omega_{\sigma\rho} = -\Delta\omega_{\rho\sigma}. \quad (17)$$

In matrix form we can write the infinitesimal Lorentz transformation as (the factor $\frac{1}{2}$ is convention in order to obtain the standard definition of the angular momentum $J_i = \frac{1}{2}\epsilon_{ijk} M^{jk}$)

$$\begin{aligned} \Lambda(\Delta\omega_{\mu\nu}) &= \mathbb{1} - \frac{1}{2} \Delta\omega_{\mu\nu} \hat{M}_{\mu\nu} \\ &= \mathbb{1} - \frac{1}{2} \Delta\omega_{\mu\nu} (q_\mu \partial_\nu - q_\nu \partial_\mu) \end{aligned} \quad (18)$$

where $\hat{M}_{\mu\nu} = -\hat{M}_{\nu\mu}$ are the generators of the Lorentz group and we find (compare eq. (14))

$$\begin{aligned} \Lambda(\Delta\omega_{\mu\nu}) q^\sigma &= q^\sigma - \frac{1}{2} (\Delta\omega_{\mu\sigma} - \Delta\omega_{\sigma\mu}) q_\mu \\ &= q^\sigma + \Delta\omega_\mu^\sigma q^\mu. \end{aligned} \quad (19)$$

Similar for the infinitesimal translation

$$\begin{aligned} T(\Delta a) &= \mathbb{1} - i \Delta a^\mu P_\mu \\ &= \mathbb{1} + \Delta a^\mu \partial_\mu \end{aligned} \quad (20)$$

we find:

$$q'^\nu = T(\Delta a) q^\nu = q^\nu + \Delta a^\nu. \quad (21)$$

If the system is composed of several particles we find for the generators

- for the translation group

$$P^\mu = \sum_k^N p_k^\mu, \quad (22)$$

- and for the Lorentz group ($SL(n=2, \mathbb{C}) \rightarrow \dim = 2(n^2 - 1) = 6$) :

$$M^{\mu\nu} = \sum_{k=1}^N q_k^\mu p_k^\nu - q_k^\nu p_k^\mu. \quad (23)$$

These 10 generators respect the algebra of the group which is called Poincaré algebra :

$$\begin{aligned} \{P_\mu, P_\nu\} &= 0 \\ \{M_{\mu\nu}, P_\rho\} &= g_{\mu\rho}P_\nu - g_{\nu\rho}P_\mu \\ \{M_{\mu\nu}, M_{\rho\sigma}\} &= g_{\mu\rho}M_{\nu\sigma} - g_{\mu\sigma}M_{\nu\rho} \\ &\quad - g_{\nu\rho}M_{\mu\sigma} + g_{\nu\sigma}M_{\mu\rho}. \end{aligned} \quad (24)$$

This can be directly verified by going back to the definition, eqs. (18) and (20), and calculation the brackets. The generators $M_{\mu\nu}$ and P_μ do not commute. Physically, that comes from the fact that there is a length contraction in the Lorentz boost (and a time dilatation).

The generator of a Poincaré transformation is given by the combination of that of the Lorentz transformation and of a translation

$$G = \frac{1}{2}\omega^{\mu\nu}M_{\mu\nu} - a^\mu P_\mu. \quad (25)$$

If two inertial frames \mathcal{O} and \mathcal{O}' are connected by an infinitesimal element of the Poincaré group, $R(\Lambda, a)$, then the space time coordinates of the same event in \mathcal{O} and \mathcal{O}' are related by

$$\begin{aligned} q'^\mu &= q^\mu + \{q, G\} \\ &= q^\mu + \omega^\mu_\nu q^\nu + a^\mu \\ &= \Lambda^\mu_\nu q^\nu + a^\mu. \end{aligned} \quad (26)$$

3. Reduction of the dimension of the phase space

Relativistic theories are based on 4-vectors whose transformation between two inertial systems is given by elements of the Poincaré group. This has as consequence that the phase space of a N particle system has not anymore $6N$ dimensions as in nonrelativistic dynamics but $8N$. World lines are given by $(\mathbf{q}_i(\tau), \mathbf{p}_i(\tau))$ and therefore physical trajectories (position and momentum of the particles as a function of the time τ) have $6N + 1$ dimensions. Thus we need *constraints* to reduce the number of degrees of freedom in the relativistic phase space. After a introduction to the $8N$ dimensional phase space and to the Poincaré group and algebra we will illustrate the reduction of the degrees of freedom first for the example of 1 free particle and then we extend systematically the approach to N -interacting particles.

C. From 1 to N-body relativistic system

1. The case of 1 free particle

We start with the most simple case of 1 free particle [20]. The Hamilton's equations for the time evolution of a nonrelativistic particle determines that trajectory in the phase space for which the energy is conserved. This

suggests to define a constraint, the mass shell constraint, which reads for a noninteracting particle as

$$K = p^\mu p_\mu - m^2 = 0. \quad (27)$$

It reduces the phase space from 8 to 7 dimensions by relating the energy of the particle with its 3-momentum (and also with its position if we include a potential). It defines therefore the 7 dimensional subspace Σ of the 8 dimensional phase space on which this condition is fulfilled. Because K is a Poincaré invariant quantity, we find

$$\{K, M_{\mu\nu}\} = 0, \quad \{K, P_\mu\} = 0. \quad (28)$$

Of course the 7 dimensional phase space region Σ is also Poincaré invariant

$$R(\Lambda, a)\Sigma = \Sigma. \quad (29)$$

The trajectory in phase space on which this constraint is satisfied is given by the solution of

$$\begin{aligned} \frac{dq(\tau)}{d\tau} &= \lambda\{q(\tau), K\} \\ \frac{dp(\tau)}{d\tau} &= \lambda\{p(\tau), K\} \end{aligned} \quad (30)$$

with the initial condition $q(0) = q_0$ and $p(0) = p_0$. λ is a free parameter. In order to associate to each value of τ *one* point in phase space $(q(\tau), p(\tau))$ or in other words in order to create a worldline a second constraint, $\chi(q^\mu, p^\mu, \tau) = 0$, has to be employed which fixes λ . It relates the time q^0 of the particle with a Lorentz invariant system time τ . This time constraint χ has been chosen quite differently in the literature, giving quite different time evolution equations. The subspace we are interested in is determined by a conserved χ and K constraint. This is expressed by

$$\frac{d\chi}{d\tau} = \frac{\partial\chi}{\partial\tau} + \lambda\{\chi(\tau), K\} = 0. \quad (31)$$

This equation determines λ

$$\lambda = -\frac{\partial\chi}{\partial\tau}\{\chi, K\}^{-1}. \quad (32)$$

λ depends therefore on the choice of the constraint χ . Formally we can define

$$\mathcal{Z} = \lambda K = -\frac{\partial\chi}{\partial\tau}\{\chi, K\}^{-1}K \quad (33)$$

and obtain a time evolution equation for a phase space function f

$$\begin{aligned} \frac{df}{d\tau} &= \frac{\partial f}{\partial\tau} + \lambda\{f, K\} \\ &= \frac{\partial f}{\partial\tau} + \{f, \mathcal{Z}\} \end{aligned} \quad (34)$$

which is formally identical with the nonrelativistic evolution eq. (3) but \mathcal{Z} is not the classical Hamiltonian, it is given by eq. (33).

How to treat a Hamilton system with constraints has been developed by Dirac [21]. To determine the time evolution for any function of the phase space variables along the trajectory determined by the two constraints $\phi_1 = K$ and $\phi_2 = \chi$ is given by the Dirac bracket which is defined as

$$\{A, B\}_D = \{A, B\} - \{A, \phi_i\} C_{ij} \{\phi_j, B\}, \quad (35)$$

with the matrix of these constraints

$$C_{ij}^{-1} = \{\phi_i, \phi_j\}. \quad (36)$$

On the hypersurface, where the constraints are fulfilled, Dirac brackets and Poisson brackets agree. Dirac introduced the symbol \approx to describe $\{A, B\}_D \approx \{A, B\}$ that two functions are identical at the subspace which is defined by the constraints. For our example we find

$$\begin{aligned} \{A, B\}_D = \{A, B\} &- \frac{\{A, K\}\{\chi, B\}}{\{K, \chi\}} \\ &- \frac{\{A, \chi\}\{K, B\}}{\{\chi, K\}}. \end{aligned} \quad (37)$$

The Dirac brackets of the 10 generators of the Poincaré group yield the same result as the Poisson brackets, eq. (24), because K commutes with them. Therefore we can use also the Dirac brackets to construct a transformation between the two inertial systems \mathcal{O} and \mathcal{O}' . This transformation we call $R^*(\Lambda, a)$. Both transformations, $R(\Lambda, a)$ as well as $R^*(\Lambda, a)$, map therefore Σ to Σ but $R^*(\Lambda, a)$ and $R(\Lambda, a)$ map the same point in \mathcal{O} to different points in \mathcal{O}' . Because $\{G, \chi\}_D = 0$, χ is unchanged under a transformation $R^*(\Lambda, a)$ and the Dirac brackets transform a phase space point on \mathcal{O} to a phase space point on \mathcal{O}' which has the same value of τ . For the transformation using Poisson brackets this is generally not the case. Therefore the Dirac brackets are the proper tool to determine world lines in the two inertial frames [22]. Using eq. (26) and replacing the Poisson bracket $\{\cdot, \cdot\}$ by the Dirac bracket $\{\cdot, \cdot\}_D$ we find the *canonical* transformation between two inertial systems

$$q'^\mu(\tau) = q^\mu(\tau) + \{q^\mu(\tau), G\}_D \quad (38)$$

where G is given by eq. (25). If we use the Poisson brackets for the transformation between the two inertial systems we obtain the *geometrical* transformation

$$\begin{aligned} q'^\mu(\tau) &= q^\mu(\tau + \Delta\tau) + \{q^\mu(\tau + \Delta\tau), G\} \\ &\approx q^\mu(\tau) + \frac{dq^\mu}{d\tau} \Delta\tau + \{q^\mu(\tau), G\}. \end{aligned} \quad (39)$$

Applying the general eq. (37) we can relate $\{q^\mu, G\}_D$ and $\{q^\mu, G\}$ ($\{K, G\} = 0$):

$$\{q^\mu, G\}_D = \{q^\mu, G\} - \frac{\{q^\mu, K\}\{\chi, G\}}{\{K, \chi\}}. \quad (40)$$

Using furthermore the time evolution eq. (34) we find

$$\frac{dq^\mu}{d\tau} = -\frac{\partial\chi}{\partial\tau} \frac{\{q^\mu, K\}}{\{\chi, K\}} \quad (41)$$

and therefore eq. (40) can be rewritten in the form

$$\{q^\mu, G\}_D = \{q^\mu, G\} - \{\chi, G\} \left(\frac{\partial\chi}{\partial\tau}\right)^{-1} \frac{dq^\mu}{d\tau}. \quad (42)$$

Consequently, if we can ensure that

$$\{\chi, G\} \left(\frac{\partial\chi}{\partial\tau}\right)^{-1} = \Delta\tau \quad (43)$$

the transformation between two inertial systems using Dirac brackets (the canonical transformation, eq. (38)) becomes identical to that using Poisson brackets (the geometrical transformation eq. (39)). If the condition (43) is fulfilled the world lines of particles remain the same under the two transformations. They are therefore frame independent. This requirement of the frame independence of the trajectories is called the World Line Condition (WLC).

The constraint χ determines the time evolution of the system. If we impose the constraint $\chi = q^0 - \tau = 0$ [20] we find for the time evolution of q^μ eq. (41)

$$\frac{dq^\mu}{d\tau} = \lambda\{q^\mu, K\} = \frac{p^\mu}{p^0} \quad (44)$$

whereas for the condition $\chi = x_\mu p^\mu - m\tau = 0$ [23] we obtain

$$\frac{dq^\mu}{d\tau} = \lambda\{q^\mu, K\} = \frac{p^\mu}{m}. \quad (45)$$

In both cases we have $dp^\mu/d\tau = 0$ compatible with the fact that we have a single free particle. The different time evolution equations remind us that τ is a parameter introduced by the constraint χ and not an independently defined time. Thus the time evolution of a relativistic system is only determined after the constraint χ is imposed. Different choices of the constraint yield a different time evolution of the system.

Now we come back to the question whether we can find a time evolution equations for a relativistic system which resembles the form of the time evolution equations found in non-relativistic systems

$$\begin{aligned} \frac{dq^\mu}{d\tau} &= \{q^\mu, \mathcal{H}\}_D = \lambda\{q^\mu, K\} \\ \frac{dp^\mu}{d\tau} &= \{p^\mu, \mathcal{H}\}_D = \lambda\{p^\mu, K\}. \end{aligned} \quad (46)$$

where $\mathcal{H} \neq \lambda K = \mathcal{Z}$. This can be done using the method described in [24]. Anyway it is always possible to find back such a definition using the classical limit of the relativistic equations of motion.

2. Extension to 2 interacting particles

The above discussed construction of world lines on which a particle moves independent of the chosen reference system has been extended to a larger number of particles in [20, 23, 24]. For a system with two interacting particles [22] the mass shell constraints eq. (27) have the form

$$\begin{aligned} K_1 &= p_1^\mu p_{1\mu} - m^2 + V = 0 \\ K_2 &= p_2^\mu p_{2\mu} - m^2 + V = 0 \end{aligned} \quad (47)$$

in order to have reference frame independent world lines. In addition, they have to be *first class* constraints in the notation of Dirac [21] :

$$\{K_1, K_2\} = 2 \left(p_1^\mu \frac{\partial}{\partial q_1^\mu} - p_2^\mu \frac{\partial}{\partial q_2^\mu} \right) V = 0, \quad (48)$$

a condition which can be fulfilled if the potential V depends on q_T^μ [20] which is the part of $q^\mu = q_1^\mu - q_2^\mu$ which is transverse with respect to the centre of mass motion $P^\mu = p_1^\mu + p_2^\mu$, and which is defined as

$$q_T^\mu = q^\mu - \frac{q_\nu P^\nu}{P^2} P^\mu. \quad (49)$$

Poincaré transformations map the $7N$ dimensional phase space, on which the constraints eq. (47) are fulfilled, on itself. The evolution equations can be extended to

$$\begin{aligned} \frac{dq_i^\mu}{d\tau} &= v_1 \{q_i^\mu, K_1\} + v_2 \{q_i^\mu, K_2\} \\ \frac{dp_i^\mu}{d\tau} &= v_1 \{p_i^\mu, K_1\} + v_2 \{p_i^\mu, K_2\} \end{aligned} \quad (50)$$

with arbitrary parameters v_1 and v_2 . For an interacting system the time components of particles q_i^0 become connected by the potential term and consequently the spatial position of each of the particle q_i^k depends on both times q_1^0 and q_2^0 . This does not correspond to a world line but to a sheet. To obtain a world line we have to synchronize first the times of both particles by a constraint without any parameter

$$\chi_1(q_1, q_2, p_1, p_2) = 0 \quad (51)$$

and finally to connect the synchronized times to a clock time τ

$$\chi_2(q_1, q_2, p_1, p_2, \tau) = 0 \quad (52)$$

with the property $\det\{K_i, \chi_j\} \neq 0$. If $\{K_i, \chi_j\} = 0$ we cannot assign to each point on the trajectory uniquely a value of the parameter τ . With these two additional constraints which reduce the $7N$ dimensional phase space to a $6N$ dimensional phase space with a parameter τ so effectively to a $6N + 1$ dimensional phase space [25]). Condition 52 allows for fixing the free parameters v_i of eq. 50 (see eq. 34).

$$\frac{d\chi_2(\tau)}{d\tau} = \frac{\partial\chi_2(\tau)}{\partial\tau} + \{\chi_2(\tau), K_i\}v_i = 0 \quad (53)$$

yields

$$v_i = -\{\chi_2(\tau), K_i\}^{-1} \frac{\partial\chi_2(\tau)}{\partial\tau}. \quad (54)$$

Consequently, the general evolution equation for a phase space function f is

$$\frac{df}{d\tau} = \frac{\partial f}{\partial\tau} - S_{i2} \frac{\partial\chi_2}{\partial\tau} \{f, K_i\}. \quad (55)$$

with

$$S_{ij} = \{\chi_j, K_i\}^{-1}. \quad (56)$$

As in the one particle case this requires that the two transformations between the inertial systems, the one expressed by Dirac brackets (canonical transformation)

$$q_i'^\mu(\tau) = q_i^\mu(\tau) + \{q_i^\mu(\tau), G\}_D \quad (57)$$

and the one expressed by Poisson brackets (geometrical transformation)

$$\begin{aligned} q_i'^\mu(\tau) &= q_i^\mu(\tau + \Delta\tau_i) + \{q_i^\mu(\tau + \Delta\tau_i), G\} \\ &\approx q_i^\mu(\tau) + \frac{dq_i^\mu}{d\tau} \Delta\tau_i + \{q_i^\mu(\tau), G\} \end{aligned} \quad (58)$$

lead to points on the same world lines. Employing the Dirac brackets and taking advantage of $\{K_i, G\} = 0$ we find

$$\begin{aligned} \frac{dq_i^\mu(\tau)}{d\tau} \Delta\tau_i &= \{q_i^\mu(\tau), K_j\} S_{lj} \{\chi_l, G\} \\ &= \{q_i^\mu(\tau), K_j\} S_{lj} \frac{d\chi_l}{d\tau} \Delta\tau_i, \end{aligned} \quad (59)$$

or if $\{q_i^\mu(\tau), K_j\} \neq 0$ and $S_{lj} \neq 0$

$$\{\chi_l, G\} = \frac{d\chi_l}{d\tau} \Delta\tau_i. \quad (60)$$

In reality the last equation poses two conditions: $\Delta\tau_1 = \Delta\tau_2$ and that χ_1 which does not depend on τ is Poincaré invariant to fulfill $\{\chi_l, G\} = 0$. These conditions cannot be fulfilled by every choice of χ_i . Indeed, if we relate the τ to the fourth component of q^μ , the instant form of Dirac [21],

$$\begin{aligned} \chi_1 &= \frac{1}{2}(q_1^0 - q_2^0) = 0 \\ \chi_2 &= \frac{1}{2}(q_1^0 + q_2^0) - \tau = 0, \end{aligned} \quad (61)$$

we recover $\{\chi_l, G\} \neq 0$ and hence the no go theorem stating that relativistic molecular dynamics can only be formulated for non interacting particles [20]. If, on the other hand, the χ_i are defined kinematically as

$$\begin{aligned} \chi_1 &= \frac{1}{2} q^\mu U_\mu = 0 \\ \chi_2 &= \frac{1}{2} (q_1^\mu + q_2^\mu) U_\mu - \tau = 0 \end{aligned} \quad (62)$$

with $U_\mu = P_\mu/\sqrt{P^2}$, which gives $U_\mu = (1, \vec{0})$ in the centre of mass of two particles, the world line condition can be fulfilled [20] by setting $\Delta\tau_i = -\{\chi_2, G\}$. With the latter time constraints eq. (62), we can compute the v_i (eq. (54)). We start out from the matrix of constraints :

$$\begin{aligned} S_{ij}^{-1} &= \begin{pmatrix} \{\chi_1, K_1\} & \{\chi_1, K_2\} \\ \{\chi_2, K_1\} & \{\chi_2, K_2\} \end{pmatrix} \\ &= \begin{pmatrix} p_1^\mu U_\mu & -p_2^\mu U_\mu \\ p_1^\mu U_\mu & p_2^\mu U_\mu \end{pmatrix}, \end{aligned} \quad (63)$$

which can be inverted :

$$S_{ij} = \begin{pmatrix} (2 p_1^\mu U_\mu)^{-1} & (2 p_1^\mu U_\mu)^{-1} \\ -(2 p_2^\mu U_\mu)^{-1} & (2 p_2^\mu U_\mu)^{-1} \end{pmatrix}. \quad (64)$$

The parameter v_i becomes

$$\begin{aligned} v_1 &= (2 p_1^\mu U_\mu)^{-1} \stackrel{\text{cms}}{=} \frac{1}{2E_1} \\ v_2 &= (2 p_2^\mu U_\mu)^{-1} \stackrel{\text{cms}}{=} \frac{1}{2E_2} \end{aligned} \quad (65)$$

and we obtain finally the equations of motion for 2 interacting particles in their center of mass

$$\begin{aligned} \frac{\partial q_i^\mu}{\partial \tau} &= \frac{p_i^\mu}{E_i} \\ \frac{\partial p_i^\mu}{\partial \tau} &= - \sum_{k=1}^2 \frac{1}{2E_k} \frac{\partial V(q_T)}{\partial q_{i\mu}}. \end{aligned} \quad (66)$$

We can easily see that the classical non-relativistic limit of these equations gives the same result as QMD by taking $\mathbf{p} \ll m$.

In this example of two interacting particles we can also address another problem which is the *separability* of clusters. In contradiction to nonrelativistic dynamics this separability is not trivially fulfilled by taking a vanishing potential for large distances because the potential enters the constraint matrix which determines the time evolution. Cluster separability means that we have the equations of motion of two free particles if the distance between them is large.

3. Extention of the formalism

In order to define world lines for relativistic particles we have to reduce the relativistic phase space from $8N$ dimensions to $6N+1$ dimensions. This is done by relating the zero component of the space time and of the energy momentum 4-vector, (q_i^0, p_i^0) , to the vector parts of these 4-vectors with help of constraints. In addition we have to introduce a system time τ which describes the evolution of the system.

For the two body case, for which $\{K_i, K_j\} = 0$, the formalism has been developed in the last subsection. Here we extend the formalism to $N > 2$ where $\{K_i, K_j\}$ may

be different from 0. In this case the time evolution equations for the $2N$ constraints are

$$\begin{aligned} \frac{d\phi_i}{d\tau} &= \frac{\partial \phi_i}{\partial \tau} + \sum_k^{2N} \lambda_k \{\phi_i, \phi_k\} = 0 \\ &= \frac{\partial \phi_i}{\partial \tau} + \sum_k^{2N} \lambda_k C_{ik}^{-1} = 0. \end{aligned} \quad (67)$$

with

$$\phi_k = \begin{cases} K_k(q^\mu, p^\mu) = 0 \text{ for } 1 < k < N \\ \chi_k(q^\mu, p^\mu) = 0 \text{ for } N+1 < k < 2N-1 \\ \chi_N(q^\mu, p^\mu, \tau) = 0. \end{cases} \quad (68)$$

Only the constraint $i = 2N$ depend on τ . Rewriting the last line of eq. (67) as

$$\sum_k^{2N} \lambda_k C_{ik}^{-1} = a_i \quad (69)$$

with a_i being a vector in which only the $2N^{th}$ component is different from zero we find

$$\lambda_k = -C_{ik} a_i = -\frac{\partial \phi_N}{\partial \tau} C_{2Nk}. \quad (70)$$

Also this equation shows that different choices of constraints will yield different values of λ_k and different λ_k will give a different time evolution. Therefore the relativistic kinematics is only defined after the constraints are defined. This will be discussed in the next subsection. Defining

$$\mathcal{Z} = \sum_k^{2N} \lambda_k \phi_k \quad (71)$$

the trajectory in phase space for which the constraints are fulfilled are given by

$$\begin{aligned} \frac{dq_i^\mu}{d\tau} &= \{q_i^\mu(\tau), \mathcal{Z}\} \\ \frac{dp_i^\mu}{d\tau} &= \{p_i^\mu(\tau), \mathcal{Z}\}. \end{aligned} \quad (72)$$

and have therefore the form of which reminds us on the Hamilton-Jacobi equations. This can be easily understood by recalling that the non-relativistic equations of motion lead to a trajectories on which the total energy of the system is conserved whereas the eqs. (72) lead to trajectories on which the constraints ϕ_k are conserved.

4. N-particle system

The N-body system is actually a trivial generalization of the 3-body problem. Therefore we will discuss here the 3-body case which was studied in detail in [15, 20, 24]. As compared to the 2-body case we are confronted here with several new features:

- even if we know that the WLC imposes that exactly one of the χ_i has to depend on τ , we don't know their definition and there are several possibilities that we will discuss,
- the commutation of the on-shell mass constraints $\{K_i, K_j\}$ which is easily fulfilled in the 2 particle case (eq. (48)), and which avoids that χ constraints appear explicitly in the equations of motion, is not necessarily fulfilled for the 3 particle case.
- we still have to respect the WLC and the cluster separability.

We start out with the definition of some useful quantities. First of all we define the frame *projectors* (this name is used in [26]) :

$$u_{ij}^\mu = \frac{p_{ij}^\mu}{\sqrt{p_{ij}^2}} \stackrel{\text{cms}}{=} (1, 0, 0, 0) \quad (73)$$

where $p_{ij}^\mu = p_i^\mu + p_j^\mu$ and

$$U^\mu = \frac{P^\mu}{\sqrt{P^2}} \stackrel{\text{lab}}{=} (1, 0, 0, 0) \quad (74)$$

where P^μ is the Poincaré generator (22). We call the latter system laboratory system because in the collider physics the total center of mass system is identical to the laboratory system.

These projectors are used to select the 4th component of 4-vector in the desired frame. Here u_{ij}^μ is the projector for the centre of mass (cms) of two particles i and j , and U^μ is the center of mass of for the whole N-particle system (lab system). The derivatives of these quantities are :

$$\begin{aligned} \frac{\partial u_{ij}^\mu}{\partial q_k^\nu} &= 0 \\ \frac{\partial u_{ij}^\mu}{\partial p_k^\nu} &= \frac{1}{\sqrt{p_{ij}^2}} (g^{\mu\nu} - u_{ij}^\mu u_{ij}^\nu) (\delta_{ik} + \delta_{jk}) \end{aligned} \quad (75)$$

and

$$\begin{aligned} \frac{\partial U^\mu}{\partial q_k^\nu} &= 0 \\ \frac{\partial U^\mu}{\partial p_k^\nu} &= \frac{1}{\sqrt{P^2}} (g^{\mu\nu} - U^\mu U^\nu). \end{aligned} \quad (76)$$

We can define

$$\theta^{\mu\nu} = (g^{\mu\nu} - u_{ij}^\mu u_{ij}^\nu) \stackrel{\text{cms}}{=} \begin{pmatrix} 0 & 0 & 0 & 0 \\ 0 & -1 & 0 & 0 \\ 0 & 0 & -1 & 0 \\ 0 & 0 & 0 & -1 \end{pmatrix} \quad (77)$$

and

$$\Theta^{\mu\nu} = (g^{\mu\nu} - U^\mu U^\nu) \stackrel{\text{lab}}{=} \begin{pmatrix} 0 & 0 & 0 & 0 \\ 0 & -1 & 0 & 0 \\ 0 & 0 & -1 & 0 \\ 0 & 0 & 0 & -1 \end{pmatrix}, \quad (78)$$

for a more compact notation. These projectors allow for defining two transverse distances :

$$\begin{aligned} q_{Tij}^\mu &= q_{ij}^\sigma \theta_{\sigma\mu} \\ &= q_{ij}^\mu - ((q_{ij})_\sigma u_{ij}^\sigma) u_{ij}^\mu \\ q_{Tij}^2 &= q_{ij}^2 - ((q_{ij})_\sigma u_{ij}^\sigma)^2 \end{aligned} \quad (79)$$

and

$$\begin{aligned} q'_{Tij}{}^\mu &= q_{ij}^\sigma \Theta_{\sigma\mu} \\ &= q_{ij}^\mu - ((q_{ij})_\sigma U^\sigma) U^\mu, \\ q'_{Tij}{}^2 &= q_{ij}^2 - ((q_{ij})_\sigma U^\sigma)^2. \end{aligned} \quad (80)$$

We notice the following properties :

$$\begin{aligned} (q_{Tij})_\mu u_{ij}^\mu &= 0 \\ (q_{Tij})_\mu \theta^{\mu\nu} &= q_{Tij}^\nu \end{aligned} \quad (81)$$

and

$$\begin{aligned} (q'_{Tij})_\mu U^\mu &= 0 \\ (q'_{Tij})_\mu \Theta^{\mu\nu} &= q'_{Tij}{}^\nu. \end{aligned} \quad (82)$$

The derivatives of these transverse distances are relegated to appendix 1a.

We start the discussion of the 3-particles dynamics with the proposition of the constraints made in the Relativistic Quantum Molecular Dynamics (RQMD) of ref. [15]. In this paper the authors extend the previously discussed 2-body system to a N-body system and employ as mass shell constraints including the potential V

$$K_i = p_i^\nu p_{i\nu} - m_i^2 + V_i(q_{Tij}^2) = 0. \quad (83)$$

In the same way the time constraints are defined by

$$\chi_i = \frac{\sum_{j \neq i} q_{ij}^\nu}{N} (u_{ij})_\nu = 0 \quad ; \quad 1 \leq i \leq N-1. \quad (84)$$

These constraints connect times between couples of particles. The last constraint

$$\chi_N = \frac{\sum_j q_j^\nu}{N} U_\nu - \tau = 0 \quad (85)$$

ensures that all times are related to the time evolution parameter τ .

All these constraints fulfil the WLC [15]. In order to assure the separability of clusters two particle distances are weighted with the weighting function

$$g_{ij} = \frac{L}{q_{Tij}^2} \exp\left(\frac{q_{Tij}^2}{L}\right). \quad (86)$$

There are several problems with this approach. The first is that the Komar-Todorov (KT) [26] condition, $\{K_i, K_j\} = 0$, is not fulfilled. This means that the mass

shell constraints of the different particles are not independent.

$$\begin{aligned}\{K_i, K_j\} &= 2p_j^\mu \frac{\partial V_i}{\partial q_j^\mu} - 2p_i^\mu \frac{\partial V_j}{\partial q_i^\mu} + \{V_i, V_j\} \\ &= 2p_{ij}^\mu \frac{\partial V_i}{\partial q_j^\mu} + \{V_i, V_j\} \neq 0\end{aligned}\quad (87)$$

using the fact that $\partial V_i / \partial q_j^\mu = -\partial V_j / \partial q_i^\mu$. We notice that neither $V(q_T)$ nor $V(q'_T)$ can fulfil this condition. In the RQMD paper [15] it is assumed that $\{K_i, K_j\}$ remains negligible and consequently the time constraints do not appear in the full equations of motion based on eq. (72)

$$\begin{aligned}\frac{dq_i^\mu}{d\tau} &= \sum_{k=1}^N \lambda_k \frac{\partial K_k}{\partial p_{i\mu}} + \sum_{k=N+1}^{2N} \lambda_k \frac{\partial \chi_k}{\partial p_{i\mu}} \\ \frac{dp_i^\mu}{d\tau} &= -\sum_{k=1}^N \lambda_k \frac{\partial K_k}{\partial q_{i\mu}} - \sum_{k=N+1}^{2N} \lambda_k \frac{\partial \chi_k}{\partial q_{i\mu}}\end{aligned}\quad (88)$$

because if we assume $\{K_i, K_j\} = 0$, then $\lambda_k = 0$ for $N+1 < k < 2N$ (see eq. (70)). With this assumption and the time constraint eq. (84) and (85) the parameter λ becomes

$$\lambda_k = S_{Nk}, \quad (89)$$

where S_{Nk} is defined in eq. (56). The equations of motion of [15] are then given by

$$\begin{aligned}\frac{dq_i^\mu}{d\tau} &= 2p_{i\mu} S_{Ni} \\ \frac{dp_i^\mu}{d\tau} &= -\sum_{k=1}^N S_{Nk} \frac{\partial V(q_T)}{\partial q_{i\mu}}.\end{aligned}\quad (90)$$

Even if we deal with three free particles and therefore the KT condition is trivially fulfilled, the approach of ref. [15] poses problems. Taking the constraints

$$\begin{aligned}K_1 &= p_1^2 - m_1^2 = 0 \\ K_2 &= p_2^2 - m_2^2 = 0 \\ K_3 &= p_3^2 - m_3^2 = 0,\end{aligned}\quad (91)$$

for free particles and

$$\begin{aligned}\chi_1 &= (q_{12}^\mu u_{12\mu} + q_{13}^\mu u_{13\mu})/3 = 0 \\ \chi_2 &= (q_{21}^\mu u_{21\mu} + q_{23}^\mu u_{23\mu})/3 = 0 \\ \chi_3 &= (q_1 + q_2 + q_3)^\mu U_\mu / 3 - \tau = 0\end{aligned}\quad (92)$$

gives the matrix of constraints

$$S_{ij}^{-1} = \begin{pmatrix} 4/3 p_1^\mu (u_{12} + u_{13})_\mu & -2/3 p_2^\mu u_{12\mu} & -2/3 p_3^\mu u_{13\mu} \\ -2/3 p_1^\mu u_{12\mu} & 4/3 p_2^\mu (u_{21} + u_{23})_\mu & -2/3 p_3^\mu u_{23\mu} \\ 2/3 p_1^\mu U_\mu & 2/3 p_2^\mu U_\mu & 2/3 p_3^\mu U_\mu \end{pmatrix}, \quad (93)$$

whose inverse is highly non-trivial. The numerical calculation of λ_k gives non-physical trajectories with velocities above the speed of light. Moreover, if we include the weight function, eq. (86), for the separability of clusters we encounter another numerical problem : the matrix inversion fails due to the fact that the numerical values of the matrix elements cover very many orders of magnitude. This has been discussed in [27].

Last but not least the energy is not conserved locally in time (it is conserved on average over a long time) because of the use of q_T as variable of the potential. This choice imposes to compute the forces in each two body centre of masses system. Therefore an inverse Lorentz boost has to be applied to transform all forces into the same common frame. This transformation is problematic because the Lorentz transformation is not valid when we study accelerated particles and indeed creates fluctuations of the energy of the system.

To avoid these problems we made a different choice of constraints. Instead of formulating the constraint in the two body systems we define them in the common center of mass system. These means that we have to replace the

u_{ij}^μ by U^μ in the constraint formulas which then read as

$$\begin{aligned}K_i &= p_i^\nu p_{i\nu} - m_i^2 + V_i(q_T'^2) = 0 \\ \chi_i &= \frac{\sum_{j \neq i} q_{ij}^\nu}{N} U_\nu = 0 \\ \chi_N &= \frac{\sum_j q_j^\nu}{N} U_\nu - \tau = 0.\end{aligned}\quad (94)$$

We cannot fulfil the KT condition using q'_T (see appendix 1 b), but the weaker condition $\{K_i, \sum_{i \neq j} K_j\} = 0$. This means that the mass shell constraint of the particle i commutes with the sum of that of all other particles what is not the case in the approach of ref. [15]. Similar as in [15] we assume that $\{K_i, K_j\}$ is negligible.

Our choice of constraints avoids all the other problems of the approach of [15]. We can check that using the previous example of 3 free particles. Changing the time constraints to

$$\begin{aligned}\chi_1 &= (q_{12} + q_{13})^\mu U_\mu / 3 = 0 \\ \chi_2 &= (q_{21} + q_{23})^\mu U_\mu / 3 = 0\end{aligned}\quad (95)$$

which gives

$$S_{ij}^{-1} = \begin{pmatrix} 4/3 p_1^\mu U_\mu & -2/3 p_2^\mu U_\mu & -2/3 p_3^\mu U_\mu \\ -2/3 p_1^\mu U_\mu & 4/3 p_2^\mu U_\mu & -2/3 p_3^\mu U_\mu \\ 2/3 p_1^\mu U_\mu & 2/3 p_2^\mu U_\mu & 2/3 p_3^\mu U_\mu \end{pmatrix}, \quad (96)$$

$$S_{ij} = \begin{pmatrix} (2 p_1^\mu U_\mu)^{-1} & 0 & (2 p_1^\mu U_\mu)^{-1} \\ 0 & (2 p_2^\mu U_\mu)^{-1} & (2 p_2^\mu U_\mu)^{-1} \\ -(2 p_3^\mu U_\mu)^{-1} & -(2 p_3^\mu U_\mu)^{-1} & (2 p_3^\mu U_\mu)^{-1} \end{pmatrix}. \quad (97)$$

The last column is the λ parameter which has an analytical and trivial solution

$$\lambda_k = (2 p_k^\mu U_\mu)^{-1} \stackrel{\text{lab}}{=} \frac{1}{2E_k} \quad (98)$$

which is in perfect agreement with the solution we found for the 2-particle case. The equations of motion in the global frame (lab), where $\sum_i^N \mathbf{p}_i = 0$, are then

$$\begin{aligned} \frac{dq_i^\mu}{d\tau} &= \frac{p_i^\mu}{E_i} \\ \frac{dp_i^\mu}{d\tau} &= - \sum_{k=1}^N \frac{1}{E_i} \frac{\partial V_k(q'_T)}{\partial q_{i\mu}}. \end{aligned} \quad (99)$$

These equations conserve energy and ensure physical trajectories with velocities below the speed of light. Moreover, the analytical solution for the λ_k is useful to avoid the numerical inversion of the matrix of constraints at each time step of the evolution, what is not possible with presently available computers. The equations of motion of eqs. (99) are finally identical to the relativistic equations which are currently used in other approaches [28].

Our approach also avoids the problem of the cluster separability. This can easily be seen by dividing the system into two subsystems a and b with

$$P^\mu = P_a^\mu + P_b^\mu. \quad (100)$$

If we calculate the time evolution equations for the partons in each subsystem separately we obtain the same result as if we calculate them for the full system. This means that one cluster does not influence the motion of the other.

III. NAMBU-JONA-LASINIO MODEL

In this paper we study the expansion of a q/\bar{q} plasma employing the Nambu–Jona-Lasinio (NJL) model. The NJL model is the simplest low energy approximation of QCD. It describes the interaction between two quark currents as a point-like exchange of a perturbative gluon [29]. Assuming that the mass of the gluon is large as compared to its momentum the interaction reduces to an effective

we find the solution

four point interaction and is given by

$$\mathcal{L}^{int} = \kappa \sum_{c=1}^{N_c^2-1} \sum_{i,j}^3 (\bar{q}_{i,\alpha} [\gamma^\mu \lambda^c]_{\alpha\delta} q_{i,\delta}) (\bar{q}_{j,\gamma} [\gamma^\mu \lambda^c]_{\gamma\beta} q_{j,\beta}) \quad (101)$$

where we have explicitly shown the color/Dirac $\alpha, \beta, \gamma, \delta$ and flavor i, j indices. We normalize $\sum_{i=0}^8 \lambda_{\alpha\beta}^i \lambda_{\beta\alpha}^i = 2$. Applying a Fierz transformation in color space to this interaction the Lagrangian separates into two pieces [30]: an attractive color singlet interaction between a quark and an antiquark ($\mathcal{L}_{(q\bar{q})}$) and a repulsive color anti-triplet interaction between two quarks ($\mathcal{L}_{(qq)}$) which disappears in the large N_c limit. Usually a six point interaction in the form of the 't Hooft determinant is added (\mathcal{L}_A) to break the unwanted $U_A(1)$ symmetry of the Lagrangian. For this study we are only interested in the color singlet channel (the color octet channel gives diquarks and can be used to study baryons [31, 32]):

$$\mathcal{L} = \mathcal{L}_0 + \mathcal{L}_{(q\bar{q})} + \mathcal{L}_A. \quad (102)$$

\mathcal{L}_0 is the Lagrangian for a particle without interaction. Concentrating on the dominant scalar and pseudo scalar part in Dirac space we find the following explicit form of the Lagrangian:

$$\begin{aligned} \mathcal{L} = & \sum_{f=\{u,d,s\}} \left[\bar{q}_f (i\not{\partial} - m_f^0) q_f \right. \\ & + G_S \sum_{a=0}^8 [(\bar{q}_f \lambda_F^a q_f)^2 + (\bar{q}_f i\gamma_5 \lambda_F^a q_f)^2] \\ & \left. - G_D [\det[\bar{q}_f (1 - \gamma_5) q_f] + \det[\bar{q}_f (1 + \gamma_5) q_f]] \right]. \end{aligned} \quad (103)$$

The first term is the free kinetic part, including the flavor dependent current quark masses m_f^0 which break explicitly the chiral symmetry of the Lagrangian. The second part is the scalar/pseudoscalar interaction in the mesonic channel, invariant under $SU_A(3) \otimes U_A(1)$. It is diagonal in color as the third part, the 't Hooft determinant. The det runs over the flavor degrees of freedom. Consequently the flavors become connected. G_S is the $q\bar{q}$ coupling constant and G_D the coupling constant of the 't Hooft term. The quarks in the NJL Lagrangian have four point interactions (with a coupling constant G_S) and 6 point interactions (with a coupling constant G_D).

The thermodynamic properties if this Lagrangian are summarized in ref. [11]. The NJL Lagrangian has been discussed in many review articles [29, 33, 34] where all details of this model can be found. We concentrate here on those quantities which enter directly in our calculation, the quark and meson masses as well as the cross sections.

A. Quark Masses

In the NJL model the mass of a free quark of flavor i is given by [29]

$$m_i = m_i^0 + G_S(4N_c)(i\text{Tr } S_i) - G_D(2N_c^2 + 3N_c + 1)(i\text{Tr } S_j)(i\text{Tr } S_k), \quad (104)$$

where m_i^0 is the bare mass of quark, N_c is the number of colors, with $i \neq j \neq k$ and

$$\begin{aligned} \text{Tr } S_k &= \text{Tr } S_k(x=0) \\ &= \int^\Lambda \frac{d^4 p}{(2\pi)^4} \text{Tr } S_k(p) \\ &= \int^\Lambda \frac{d^4 p}{(2\pi)^4} \text{Tr } \frac{1}{\not{p} - m_k + i\epsilon} \\ &= \frac{2}{i} \int^\Lambda \frac{d^3 p}{(2\pi)^3} \frac{m_k}{E_p} \end{aligned} \quad (105)$$

with $E_p = \sqrt{\mathbf{p}^2 + m_k^2}$. We use here a 3-momentum cut-off to regularize the integrals. If the quark is brought into matter with a finite baryon density μ and a finite temperature T thermal field theory has to be employed and we have to replace

$$p = (p_0, \mathbf{p}) \rightarrow p_n = (i\omega_n \pm \mu, \mathbf{p})$$

$$i \int^\Lambda \frac{d^4 p}{(2\pi)^4} \rightarrow -T \sum_n \int^\Lambda \frac{d^3 p}{(2\pi)^3} \quad (106)$$

where $\omega_n = (2n+1)\pi T$ with $n = 1, 2, \dots$ are the Matsubara frequencies for fermions. Hence we find for the propagator

$$\begin{aligned} S(p) &\rightarrow S(\omega_n, \mathbf{p}) = \frac{1}{\not{p}_n - m + \gamma^0 \mu} \\ &= \frac{\not{p} + m}{2E_p} \frac{1}{i\omega_n - (E_p - \mu)} \\ &\quad + \frac{\not{p}' - m}{2E_p} \frac{1}{i\omega_n + (E_p + \mu)} \end{aligned} \quad (107)$$

with

$$\not{p} = \gamma^0 E_p - \boldsymbol{\gamma} \mathbf{p} \quad (108)$$

and

$$\not{p}' = \gamma^0 E_p + \boldsymbol{\gamma} \mathbf{p}. \quad (109)$$

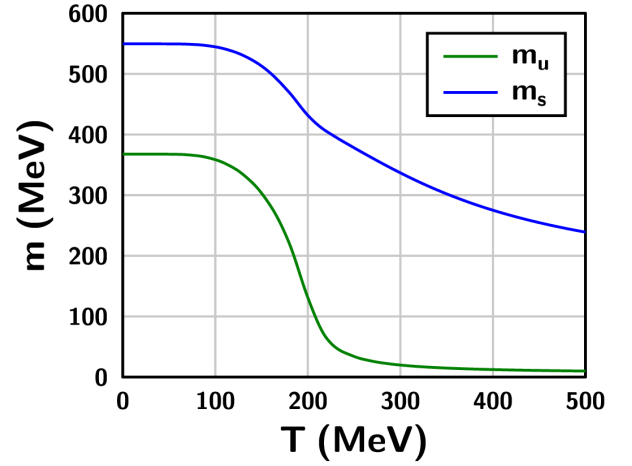


FIG. 1: Masses of u and s quarks as a function of T .

This yields [29]

$$\text{Tr } S_k = \frac{2}{i} \int^\Lambda \frac{d^3 p}{(2\pi)^3} \frac{m}{E_p} [1 - f(E_p - \mu) - f(E_p + \mu)] \quad (110)$$

with the Fermi-Dirac distribution

$$f(E_p \pm \mu) = [1 + \exp((E_p \pm \mu)/T)]^{-1}. \quad (111)$$

Eq. (104) allows then to calculate the quark masses which are displayed on Fig. 1.

B. Meson Masses and Coupling Constants

How appear mesons in a theory whose Lagrangian has only quarks as degrees of freedom? This is shown in Fig. 2. It displays the scattering of a quark and an antiquark in our theory with 4-point interactions. The left hand side displays the series of the exchange terms which appear in the the random phase approximation. This series can be summed up. The sum is formally displayed on the right hand side of this figure. This sum corresponds in leading order of N_c to the propagator of a meson with the proper quantum numbers.

The central building block for the random phase approximation is the quark-antiquark polarization propagator (Fig. 3)

$$\begin{aligned} \frac{1}{i} \left[\Pi^{P/S}(q^2, m_1, m_2) \right]_{ij} &= -N_c \sum_{f, f'} \int \frac{d^4 p}{(2\pi)^4} \text{Tr} \\ &\quad \gamma_5(T_i)_{ff'} S^f \left(p + \frac{1}{2} q \right) \gamma_5(T_j)_{f'f} S^{f'} \left(p - \frac{1}{2} q \right) \end{aligned} \quad (112)$$

where f and f' are the explicit flavour indices and tr refers therefore to the spinor trace only. T_i and T_j select

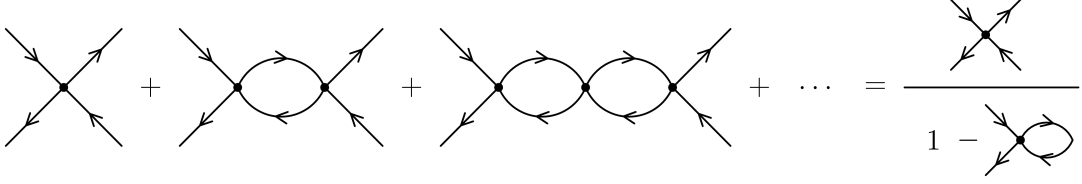


FIG. 2: Effective interaction between two quarks in Random Phase Approximation (RPA).

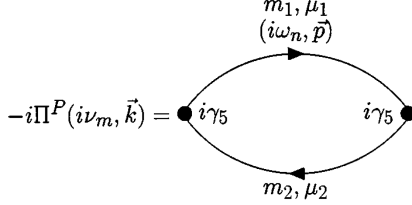


FIG. 3: The quark-antiquark polarisation propagator for pseudoscalar coupling.

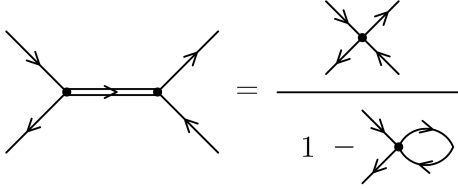


FIG. 4: The meson propagator corresponds to the RPA sum.

the appropriate flavour channel

$$T_i = \begin{cases} \lambda_3 & \text{for } \pi^0 \\ \frac{1}{\sqrt{2}}(\lambda_1 \pm i\lambda_2) & \text{for } \pi^+, \pi^- \\ \frac{1}{\sqrt{2}}(\lambda_6 \pm i\lambda_7) & \text{for } K^0, \bar{K}^0 \\ \frac{1}{\sqrt{2}}(\lambda_4 \pm i\lambda_5) & \text{for } K^+, K^-. \end{cases} \quad (113)$$

For the more complicated η and η' , where $\Pi^{P/S}$ is not diagonal, we refer to [29] where this is treated in detail. After the traces and sums of the polarization propagator eq. (112) are carried out one arrives at

$$\begin{aligned} \frac{1}{i}\Pi^{P/S}(q^2, m_1, m_2) &= 4N_c I_1(m_1) \\ &+ 4N_c I_1(m_2) \\ &- 4N_c q^2 I_2(q^2, m_1, m_2) \end{aligned} \quad (114)$$

with

$$\begin{aligned} I_1(m) &= \int \frac{d^4 p}{(2\pi)^4} \frac{1}{p^2 - m^2} \\ I_2(q^2, m_1, m_2) &= \int \frac{d^4 p}{(2\pi)^4} \frac{1}{p^2 - m^2} \\ &\quad \frac{1}{(p+q)^2 - m^2}. \end{aligned} \quad (115)$$

Having the polarisation propagator we can sum up the terms of Fig. 2. The interactions among a quark and an

antiquark with pseudoscalar coupling in random phase approximation can be written as

$$\begin{aligned} &i\gamma_5 T_k \left[2iG_S + 2iG_S \frac{1}{i} \Pi^{P/S} 2iG_S + \dots \right] i\gamma_5 T_l \\ &= i\gamma_5 T_k \frac{2iG_S}{1 - 2G_S \Pi^{P/S}} i\gamma_5 T_l. \end{aligned} \quad (116)$$

If a pseudo scalar meson with a mass M is exchanged between the quarks, Fig. 4, we find for the interaction

$$i\gamma_5 T_k \frac{-ig_{\pi q\bar{q}}^2(M)}{k^2 - M^2} i\gamma_5 T_l. \quad (117)$$

Eqs. (116) and (117) have the same structure and therefore we can identify the exchange of a pseudoscalar meson with the RPA summation of $q\bar{q}$ exchanges

$$\frac{2iG_S}{1 - 2G_S \Pi^{P/S}} = \frac{-ig_{\pi q\bar{q}}^2}{k^2 - M^2}. \quad (118)$$

The mass of the meson can be obtained by solving the equation

$$1 - 2G_S \Pi^{P/S} \big|_{k^2=M^2} = 0 \quad (119)$$

while the coupling constant $g_{\pi q\bar{q}}$ can be related to the residue of the pole. Expanding eq. (116) around its pole $k^2 = M^2$ we find

$$\frac{2iG_S}{1 - 2G_S \Pi^{P/S}} = \frac{-i \left(\frac{\partial \Pi^{P/S}}{\partial k^2} \right)^{-1} \big|_{k^2=M^2}}{k^2 - M^2}, \quad (120)$$

and therefore we can identify

$$\left(\frac{\partial \Pi^{P/S}}{\partial k^2} \right)^{-1} \big|_{k^2=M^2} = g_{\pi q\bar{q}}^2. \quad (121)$$

For finite temperature and finite chemical potential we have to replace in eq. (112) the propagators S by imaginary time propagators \mathcal{S} .

$$\begin{aligned} \Pi^{P/S}(i\nu_n, \mathbf{q}) &= N_c T \sum_{\omega} \sum_{f, f'} \int \frac{d^3 p}{(2\pi)^3} \text{Tr} \\ &\quad \gamma_5 (T_i)_{ff'} \mathcal{S}^f(\omega_l, \mathbf{p}) \\ &\quad \gamma_5 (T_j)_{f'f} \mathcal{S}^{f'}(\omega_l + \nu_n, \mathbf{p} + \mathbf{q}). \end{aligned} \quad (122)$$

The boson frequencies ν_n are even, $\nu_n = \pm 2n \pi T$, $n = 0, 1, 2, 3, \dots$, while the fermion frequencies ω_l can take

odd values only $\omega_m = \pm(2m+1)\pi T$, $m = 0, 1, 2, 3, \dots$. So in order to find the pole mass of the pseudoscalar mesons one has to calculate eq. (122) and then solve eq. (119). The mass obtained by this procedure has not to be real. Indeed, when the mass of the meson is larger

than that of its constituents the meson can decay into its constituents

After carrying out the frequency sum $\Pi^{P/S}(i\nu_n, \mathbf{q})$ can be brought as well in the form of eq. (115) with I_1 and I_2 given by

$$\begin{aligned} I_1(m) &= -i \int^\Lambda \frac{d^3p}{(2\pi)^3} \frac{1}{2E_p} [1 - f(E_p - \mu) - f(E_p + \mu)] \\ I_2(m_1, m_2) &= i \int^\Lambda \frac{d^3p}{(2\pi)^3} \frac{1}{2E_p 2E_{p+q}} \frac{f(E_p + \mu) + f(E_p - \mu) - f(E_{p+q} + \mu) - f(E_{p+q} - \mu)}{\omega + E_p - E_{p+q} + i\epsilon} \\ &\quad + i \int^\Lambda \frac{d^3p}{(2\pi)^3} \frac{1 - f(E_p - \mu) - f(E_{p+q} + \mu)}{2E_p 2E_{p+q}} \left[\frac{1}{\omega + E_p + E_{p+q} + i\epsilon} - \frac{1}{\omega - E_p - E_{p+q} + i\epsilon} \right] \end{aligned} \quad (123)$$

with $E_p = \sqrt{m_1^2 + \mathbf{p}^2}$ and $E_{p+q} = \sqrt{m_2^2 + (\mathbf{p} + \mathbf{q})^2}$. In the present approach we limit our mesons to the pseudoscalar mesons.

The model contains five parameters: the current mass of the light and strange quarks, the coupling constants G_D and G_S and the momentum cut-off Λ , are fixed by physical observables: the pion and kaon masses, the pion decay constant, the scalar quark condensate $\langle \bar{q}q \rangle$ and the mass difference between η and η' . We will employ the parameters set: $m_q^0 = 5.5$ MeV, $m_s^0 = 140.7$ MeV, $G_S/\Lambda^2 = 1.835$, $G_D/\Lambda^5 = 12.36$, $\Lambda = 602.3$ MeV. The masses for up and strange quarks, as well as for π and K for this parameter set [11, 32] are displayed in Fig. 5. We see that for small μ and T the meson masses are smaller than the masses of their constituents. For large μ and T the opposite is true. If the mass of the constituents become smaller than the meson mass the meson mass becomes complex and the meson become quasi particles. They exist in the plasma but with a life time which decreases with increasing μ and/or T (the width $\Gamma = 2G_S \Im \Pi^{P/S}$ is displayed in yellow in Fig. 5).

C. Cross sections

If created in heavy ion collisions the quark gluon plasma will expand rapidly. Therefore, not the static properties of the theory but the cross sections between constituents become dominant. In the NJL model these cross sections can be calculated via a $1/N_c$ expansion [35]. All the details can be found in [13, 35, 36]. Therefore we mention here only the essential facts.

1. Elastic Collisions

The Feynman diagrams for the $q\bar{q} \rightarrow q\bar{q}$ cross sections are displayed in Fig. 6. We see contributions from the s-channel and from the t-channel. The matrix elements

are given by

$$\begin{aligned} -i\mathcal{M}_t &= \delta_{c_1, c_3} \delta_{c_2, c_4} \bar{u}(p_3) T u(p_1) \\ &\quad [i\mathcal{D}_t^S(p_1 - p_3)] v(p_4) T \bar{v}(p_2) \\ &\quad + \delta_{c_1, c_3} \delta_{c_2, c_4} \bar{u}(p_3) (i\gamma_5 T) u(p_1) \\ &\quad [i\mathcal{D}_t^P(p_1 - p_3)] v(p_4) (i\gamma_5 T) \bar{v}(p_2) \\ -i\mathcal{M}_s &= \delta_{c_1, c_2} \delta_{c_3, c_4} \bar{v}(p_2) T u(p_1) \\ &\quad [i\mathcal{D}_s^S(p_1 + p_2)] v(p_4) T \bar{u}(p_3) \\ &\quad + \delta_{c_1, c_2} \delta_{c_3, c_4} \bar{v}(p_2) (i\gamma_5 T) u(p_1) \\ &\quad [i\mathcal{D}_u^P(p_1 + p_2)] v(p_4) (i\gamma_5 T) \bar{u}(p_3), \end{aligned} \quad (124)$$

where $p_1(p_2)$ is the momentum of the incoming $q(\bar{q})$ and $p_3(p_4)$ that from the outgoing $q(\bar{q})$. The c_i are the color indices and T are the isospin projections on the mesons. \mathcal{D}^S and \mathcal{D}^P are the meson propagators of the form

$$\mathcal{D}^{S/P} = \frac{2G_S}{1 - 2G_S \Pi^{P/S}} \quad (125)$$

with $\Pi^{P/S}$ being the polarization tensor in the pseudo-scalar/scalar channel. This cross section is displayed in Fig. 7. We see that for most of the center of mass energies this cross section is of the order of some mb. Close to the Mott transition the cross section increases dramatically to more than hundred millibarn. The reason is the s-channel in which the incoming quarks become resonant with the intermediate meson [14]. This increase we observe in all channels, see Fig. 7. This means that at the end of the expansion of the plasma, shortly before the Mott temperature T_{Mott} is reached, the system comes almost certainly to a local equilibrium. Whether at temperatures much higher than T_{Mott} a local equilibrium can be established or maintained is in view of the size of the cross section not evident. The elastic $q\bar{q}$ and $q\bar{q}$ cross sections are of the order of a couple of mb. Because they do not have a s-channel they do not increase close to T_{Mott}

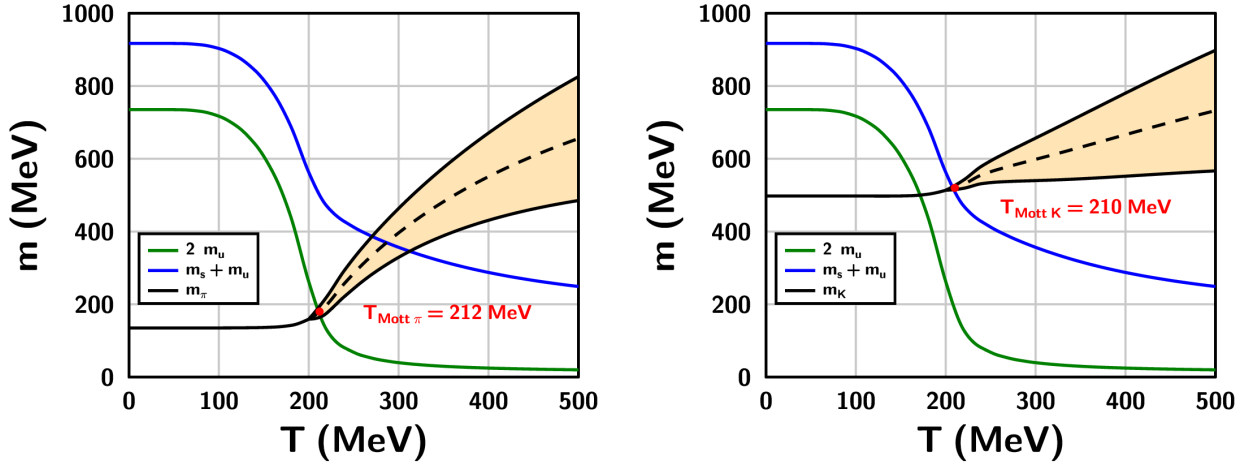


FIG. 5: Masses of π and K mesons as a function of T with the NJL model.

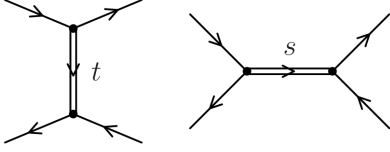


FIG. 6: The Feynman diagrams for elastic $q\bar{q}$ scattering.

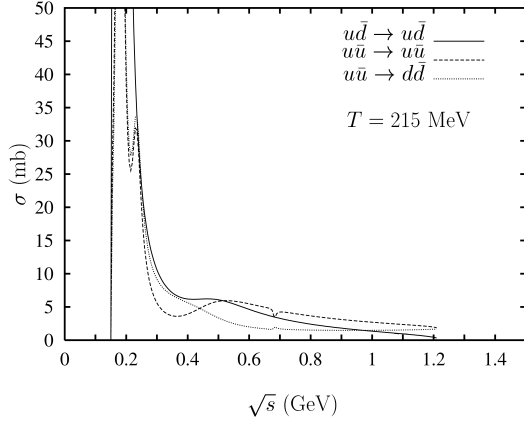


FIG. 7: Elastic cross section for the different channels as a function of \sqrt{s} for a temperature close the T_{Mott} and at $\mu = 0$ [36].

2. Hadronization Cross Section

The $1/N_c$ expansion provides as well the hadronization cross sections in which a $q\bar{q}$ pair creates two pseudoscalar mesons. The Feynman diagrams are displayed in Fig. 8. For the details of the calculation we refer to [13, 37]. Fig. 9 displays the cross section $u\bar{u} \rightarrow \pi^+\pi^-$ as a function of \sqrt{s} for different temperatures. We observe that the cross section increases close to the kinematical threshold. Close the Mott transition the cross section can reach 100 mb. Although the NJL model has no confinement this large cross section provokes that close to the cross over $q\bar{q}$

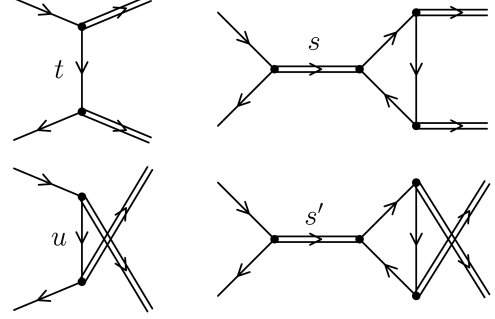


FIG. 8: The Feynman diagrams for hadronisation.

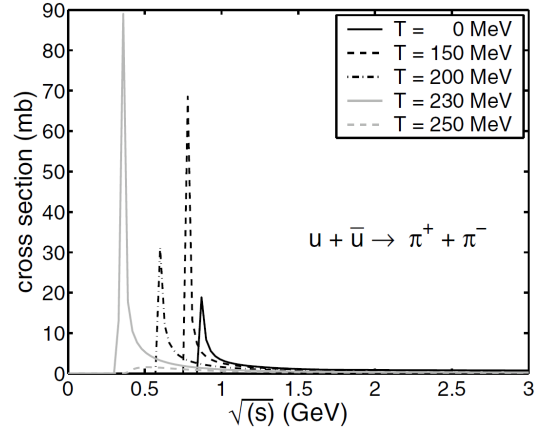


FIG. 9: Example of inelastic (right) [14] $q\bar{q}$ cross section as a function of \sqrt{s} .

pairs create mesons very effectively (the cross section for the backward reaction is kinematically suppressed) and therefore most of the quarks are converted into mesons when the system reaches the Mott transition.

We created tables of all elastic and inelastic cross sections for our simulations.

IV. SIMULATION PROGRAM

In this section we discuss how we use the results of the previous sections to formulate a molecular dynamics approach to describe the expanding q/\bar{q} plasma. The expansion of such a plasma which is presumably created in the reaction between two heavy ions at ultrarelativistic energies (at \sqrt{s} well above 10 GeV) is presently highly debated.

Hydrodynamical calculations describe the properties of particles with low transverse momentum quite reasonable, at RHIC energies ($\sqrt{s} = 200$ GeV) as well as at LHC energies ($\sqrt{s} = 2.46$ TeV). There are, as discussed in the introduction, many flavours of hydrodynamical approaches (ideal and viscous hydrodynamics, separation of core and corona, fluctuating or smoothed initial conditions, different equations of state close to hadronisation) which give very comparable results because different assumptions can have quite similar effects on observables. This makes it difficult to identify the physical processes from an agreement of the final result with the observables.

We describe the expansion in a relativistic quantum molecular dynamic approach, discussed in section 2, which is based on the NJL Lagrangian, discussed in section 3. We assume that the system remains sufficiently close to a local thermal equilibrium that we can parametrize the masses of the quarks and mesons by a local temperature and a local chemical potential. The quarks interact in two ways: Firstly, they change the mass of fellow quarks by their contribution to the chemical potential and to the local temperature, secondly, they interact with their fellow quarks by elastic and inelastic scattering. This transport approach is called INTEGRAL (INTERactive Generalized Relativistic ALgorithms).

The basic structure of a molecular dynamics program is described in the Fig. 10. We discuss in the following each of these steps.

A. Initial conditions

Principally any phase space distribution of partons can be taken as an initial condition for our calculations. In these first studies we assume a quite smooth initial distribution which is determined as follows. In a first step we calculate the radius of the colliding (identical) nuclei by

$$R = r_0 A^{1/3} \quad (126)$$

with $r_0 = 1.25$. For a finite impact parameter b we approximate the overlap region by an ellipse with the axis \mathbf{x}_E and \mathbf{y}_E :

$$\begin{aligned} \mathbf{x}_E &= R - b/2 \\ \mathbf{y}_E &= \sqrt{(R - b/2)(R + b/2)}. \end{aligned} \quad (127)$$

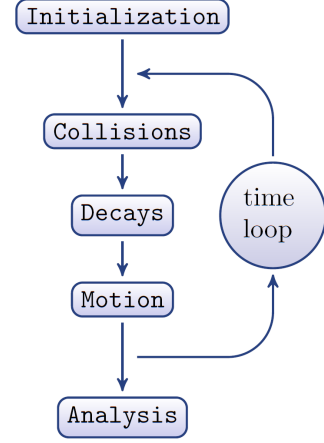


FIG. 10: Standard algorithm for molecular dynamics calculations.

The extension in the third dimension is assumed to be proportional to the creation time of the QGP. We take

$$\mathbf{z}_E = 2\tau_0 = 2 \text{ fm}. \quad (128)$$

Knowing the atomic number of the colliding nuclei, A , and the impact parameter, b , we can construct the overlap zone in coordinate space.

In the present study we assume that the system is close to local equilibrium. The mass of the partons and, consequently, their energy depends then on the local (T, μ) , which depend on the initial T_0 and μ_0 for the centre of the collision. The initial local temperature depends on the position of the parton. At a point (x, y) with $r = \sqrt{x^2 + y^2}$ the local temperature is a function of r/r_0 where the vector \mathbf{r}_0 points in the direction of \mathbf{r} and $r_0 = \sqrt{\mathbf{x}_E^2 + \mathbf{y}_E^2}$. The initial temperature is given by

$$T(r) = \frac{T_0}{1 + \exp(10 (r/r_0 - 0.8))}. \quad (129)$$

The central initial temperature T_0 can be parametrized as

$$T_0(\text{MeV}) = 68 \frac{\log(\sqrt{s_{NN}}(\text{GeV}) + 1)}{1 + \exp(1.5 (1 - \mathbf{x}_E))}. \quad (130)$$

Fig. 11 shows the initial temperature as a function of r/r_0 , Fig. 12 is a contour plot of the initial temperature. For RHIC energies this parametrization corresponds to the initial temperature of hydrodynamical calculations. Knowing the critical temperature $T_c = 165$ MeV, this equation give us for RHIC ($\sqrt{s_{NN}} = 200$ AGeV) : $T_0 \simeq 2.2T_c$, and for LHC ($\sqrt{s_{NN}} = 2760$ AGeV) : $T_0 \simeq 3.5T_c$. The calculations we present here are calculated with $\mu_0 = \mu(r) = 0$.

Knowing $(T(r), \mu = 0)$ we can determine the mass and the initial density of quarks and antiquarks.

$$\rho = \frac{N}{V} = g \int f^\pm(p) \frac{d^3p}{(2\pi)^3 (\hbar c)^3} \quad (131)$$

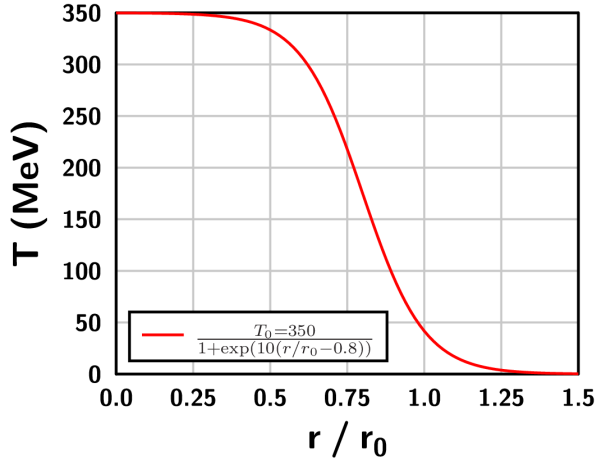


FIG. 11: Distribution of the temperature T as a function of the normalized radius r/r_0 .

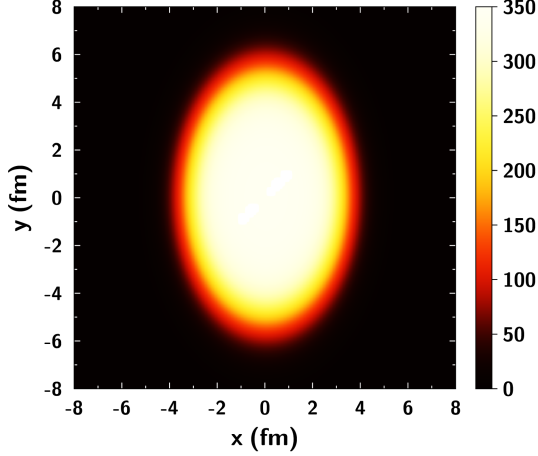


FIG. 12: Distribution of the temperature T (in MeV) in the transverse plane x, y .

where f^\pm is the Fermi-Dirac distribution (eq. 111),

$$f^\pm(p, m(T)) = \left[1 + \exp \left(\sqrt{p^2 + m^2} \pm \mu/T \right) \right]^{-1}, \quad (132)$$

g the degeneracy of the considered parton, N the quark number and V the volume in the centre of mass system of the reaction (an ellipse with constant thickness)

$$V = \pi \mathbf{x}_E \mathbf{y}_E \mathbf{z}_E. \quad (133)$$

Knowing density and volume of a slice with a given temperature we determine the local number of partons with help of eq. (129). The partons are then placed randomly in this slice. Each parton obtains its initial momentum \mathbf{p} applying a Monte Carlo procedure which models the local Fermi-Dirac distribution with (T, μ) . In the spirit of the core corona model close to the surface we assume thermalization only in longitudinal z direction and limit the transverse momentum in outward direction

by limiting the azimuthal ϕ angle. This procedure ensure that fast partons in corona are comovers and can hadronize easily. The spatial distribution of these partons is quite smooth. That is why we call this initial condition model the Hot Pancake Model (HPM).

B. Transport model

The partons in the expanding system are described by their positions and their momenta. The equations of motion of the particles are given by eq. (99)

$$\begin{aligned} \frac{dq_i^\mu}{d\tau} &= \frac{p_i^\mu}{E_i} \\ \frac{dp_i^\mu}{d\tau} &= - \sum_{k=1}^N \frac{1}{2E_k} \frac{\partial V_k(q_T)}{\partial q_{i\mu}}. \end{aligned} \quad (134)$$

In the NJL model the potential between the particles is a scalar interaction. This interaction acts like a mass which depends in our local equilibrium assumption on temperature and chemical potential of the environment. Therefore we can reformulate our energy constraints eq. (94) by

$$K_i = p_i^\mu p_{i\mu} - m_i^{*2}(T, \mu) = 0. \quad (135)$$

This modifies the equation we have to solve :

$$\frac{dp_i^\mu}{d\tau} = - \sum_{k=1}^N \frac{m_k^*}{E_k} \frac{\partial m_k^*}{\partial q_{i\mu}} \quad (136)$$

with

$$\frac{\partial m_k^*}{\partial q_{i\mu}} = \frac{\partial m_k^*}{\partial T_k} \frac{\partial T_k}{\partial q_{i\mu}} + \frac{\partial m_k^*}{\partial \mu_k} \frac{\partial \mu_k}{\partial q_{i\mu}} \quad (137)$$

and with $T_k(\mu_k)$ being the local temperature (chemical potential) of the environment of the particle k . The dependence of the mass of the partons as well as that of π 's and K 's on the chemical potential and on the temperature is displayed in Fig. 13. Here we assume that the chemical potentials of up, down and strange quarks are identical. The masses show the expected behaviour of a cross over at high T and $\mu \simeq 0$.

At high (T, μ) we see the bare mass of the partons. When approaching low (T, μ) we observe a steep rise of the mass due to the scalar potential which becomes finite. At $(T = 0, \mu = 0)$ the light partons have their constituent mass of around 370 MeV. The 't Hooft term connects up and down quarks with strange quarks. Therefore the dependence of the strange quark mass on temperature and chemical potential becomes more complex. We see a first steep rise of the mass when the chemical potential arrives from above the transition temperature of the light quarks u, d and a second rise when the genuine transition of the s quark takes place.

To solve the eqs. (99), the differential equations are converted in finite difference equations with a variable

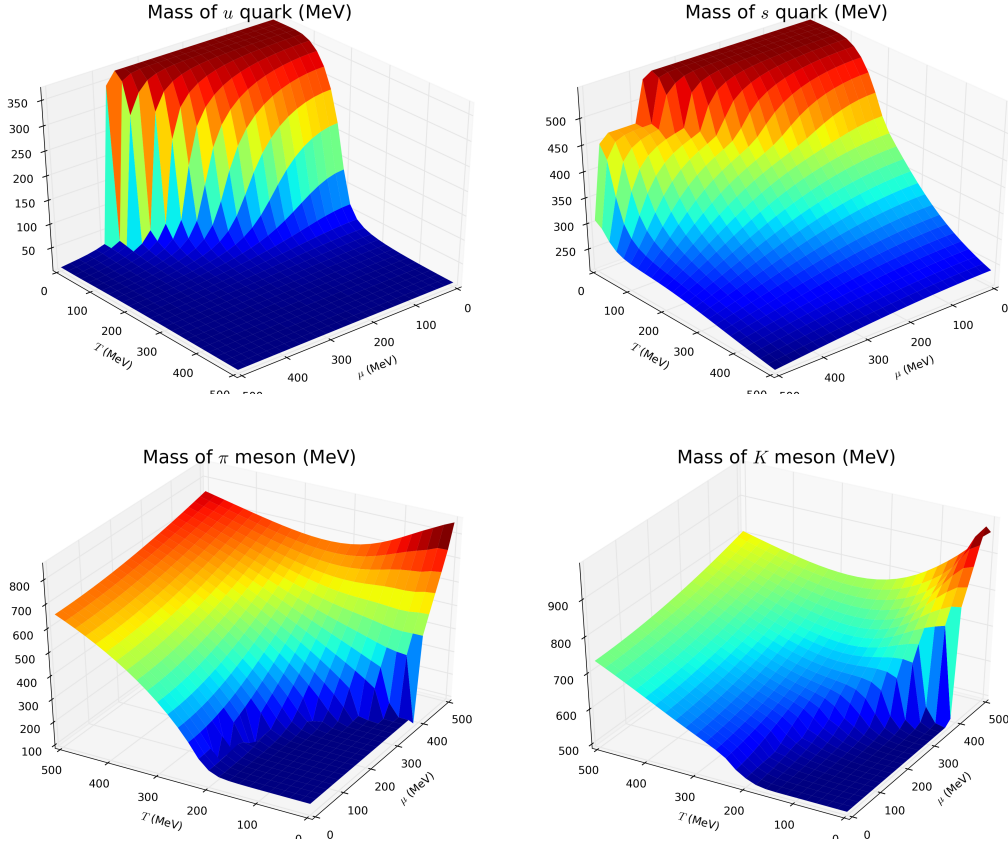


FIG. 13: Dependence of the masses on the temperature and on the chemical potential of the environment in the NJL model. In the top row we display the masses of u and s quarks, in the bottom row that of π and K mesons.

time step. Its definition will be discussed in subsection IV E. For the solution we employ an adaptive method, depending on the time step size, with either a Euler algorithm or a Runge-Kutta algorithm of second (RK2) or of forth order (RK4). The cross sections and masses which have been calculated in [32],[38] and [39] have been tabulated as a function of (T, μ, \sqrt{s}) and a linear interpolation has been applied to accelerate the calculations.

C. Thermodynamical medium

In our local equilibrium approximation the effective mass m^* of the partons depends on the temperature and chemical potential of the local environment. Therefore we have to construct these two quantities from the information on the system which is available, the 4-positions and 4-momenta of all particles. For this we define two densities, the fermionic density ρ_F and the baryonic density ρ_B

$$\rho_F(T, \mu) = \frac{N_q}{V} + \frac{N_{\bar{q}}}{V} = g \int_0^\infty \frac{d^3p}{(2\pi)^3 (\hbar c)^3} \left[2 (f^+(p, m_u) + f^-(p, m_u)) + (f^+(p, m_s) + f^-(p, m_s)) \right] \quad (138)$$

$$\rho_B(T, \mu) = \frac{N_q}{V} - \frac{N_{\bar{q}}}{V} = g \int_0^\infty \frac{d^3p}{(2\pi)^3 (\hbar c)^3} \left[2 (f^+(p, m_u) - f^-(p, m_u)) + (f^+(p, m_s) - f^-(p, m_s)) \right], \quad (139)$$

with the degeneracy factor $g = 2 \times 3 = 6$, and f^\pm defined in eq. (132). Neither ρ_F nor ρ_B are Lorentz invariants. In order to express T_i and μ_i as a function of the phase space coordinates (q_j^μ, p_j^μ) the following procedure is applied : we introduce a Lorentz invariant Gaussian function $R_{ij}(q'_T)$ inspired from the Wigner density eq. (8)

$$R_{ij}(q'_T) = \left(\frac{1}{L\sqrt{\pi}} \right)^3 \exp \left(-\frac{q'^2_{Tij}}{L^2} \right) \quad (140)$$

to calculate the contribution of a neighbouring parton j to the density of the parton i . For the width we take $L = 0.5$ fm which is about the electromagnetic radius of known hadrons. This allows for a rewriting of the density

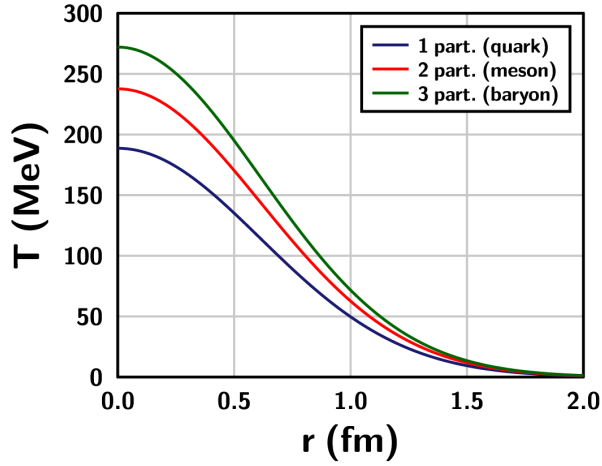


FIG. 14: Local temperature at $r = 0$ as a function the distance r and for a different number of fellow particles which have all a distance r to the considered particle.

$$\begin{aligned}\rho_{Fi} &= \sum_{j \neq i} R_{ij} \\ \rho_{Bi} &= \sum_{j \neq i} R_{ij} \text{Sign}(j),\end{aligned}\quad (141)$$

with

$$\text{Sign}(j) = \begin{cases} 1 & \text{for fermions} \\ -1 & \text{for antifermions.} \end{cases} \quad (142)$$

For $\mu = 0$ only one of these densities is necessary to determine the temperature. We use for this the Fermi density. Our approach corresponds to a Gaussian smearing of the density of a particle. These formula apply to free quarks and antiquarks. We also have to consider the partons which are bound in hadrons. For practical reasons, especially to avoid a sudden increase of the density and hence the temperature when mesons are produced, we consider mesons like one parton.

Knowing ρ_{Fi} and ρ_{Bi} , eqs. (138) and (139) allows to determine T_i and μ_i . For $\mu = 0$ and $T \gg m$ the relation between T_i and ρ_{Fi} is analytical (see appendix 2) :

$$\rho_F = \ell \frac{g}{\pi^2} \left(\frac{T}{\hbar c} \right)^3. \quad (143)$$

where $\ell = 0.90154$ being a normalization factor for the Fermi integral and the degeneracy factor becomes $g = 2 \times 2 \times 2 \times 3 \times 3 = 36$. Then we find

$$T_i = (\hbar c) \left(\frac{\pi^2}{\ell g} \right)^{1/3} \left(\sum_{j \neq i} R_{ij} \right)^{1/3}. \quad (144)$$

In the general case eqs. (138) and (139) have to be solved numerically. T_i and μ_i vary from time step to time step

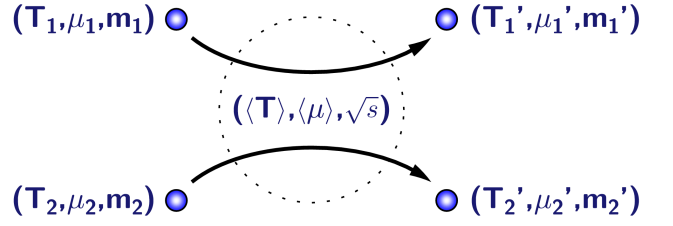


FIG. 15: Collision between 2 particles in a medium.

and therefore the mass has to be also updated in each time step for each routine (collision, decay and motion).

How the distance between particles is related to the temperature can be demonstrated assuming that there are 1, 2 or 3 particles which have an identical distance r to the considered particle. This is shown in Fig. 14. The derivatives of the temperature with respect to the phase space variables, necessary to solve eqs. (134), are developed in detail in appendix 3.

D. Cross sections and decays

In addition to the potential interaction, which generates the mass of the partons, the partons interact also by collisions. Collisions are characterized by cross sections. As in all transport theories these cross sections are converted into a geometrical concept which allows to decide which and when particles collide [16]. If two particles come closer than $\Delta r = \sqrt{\sigma/\pi}$ a collision between the particles takes place. In the program the collision is executed at that time point at which the distance between the particles is minimal.

In the present approach we have 4 types of processes :

- $q q \rightarrow q q$,
- $q \bar{q} \rightarrow q \bar{q}$,
- $q \bar{q} \rightarrow M M$ (and backward process),
- $M \rightarrow q \bar{q}$,

where quarks are characterized by q , antiquarks by \bar{q} , and mesons by M . These collisions increase the number of partons because for an expanding plasma $q \bar{q} \rightarrow M M$, in which two partons are produced, is dominating over the backward reaction. Elastic collisions are primarily responsible for the thermalization of the plasma whereas the inelastic collisions are responsible for the hadronization. Both cross sections are small at temperatures well above the Mott temperature and therefore thermalization should happen only at the last stage of the expansion of the plasma shortly before the system hadronizes.

Fig. 15 and 16 show a schema of a binary collision and a decay. The environment of both particles which enter a collision may be different and therefore we do not expect the same T and μ for both particles. In order to

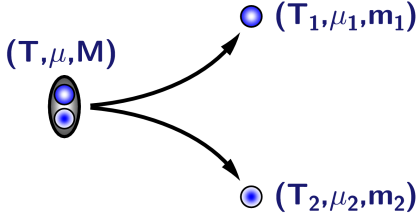


FIG. 16: Decay of a meson in a medium.

determine the cross section which depends on T and μ we average over both particles.

In the NJL approach quarks are not confined. Nothing prevents them from expanding into the vacuum. Nevertheless, applying our cross sections to the expanding system we find that at the end of the expansion almost all partons are bound in hadrons. The reason for this is the very large cross section for hadronization close to T_c . Hence, when the system expands, close to T_c hadron production becomes important. Hadrons formed slightly above T_c live sufficiently long to survive until the system has passed T_c and they become stable.

E. Mean free path and time interval

The geometrical interpretation of the cross section requires a careful study of the time step of the simulation. This can be seen by performing calculations in a box with periodic boundary conditions. As shown in Fig. 17 for the same initial condition (size of the box : $a = 3$ fm, filled with 30 free particles, for a duration of 10 fm/c) the total number of collisions depends on the chosen time step. On the top (bottom) we see the total number of collisions performed in the simulation program for the same initial condition as a function of the time step $\Delta\tau$ and for a total cross section of 1 (5) mb. We miss collisions if the time step is above a critical value of $\Delta\tau$.

The reason for this observation is that if the mean free path is smaller than the time step, it is possible to have more than 1 collision per time step for the same particle, but numerically we only apply the first collision. Therefore the time step must be smaller than the mean free path. In our simulations the time between two collisions is given by the mean free path ℓ

$$\Delta\tau = \ell = (\sigma \rho)^{-1}, \quad (145)$$

which yields

- $\Delta\tau = 10$ fm/c for $\sigma = 1$ mb,
- $\Delta\tau = 2$ fm/c for $\sigma = 5$ mb.

Fig. 17 show that in order to have the correct number of collisions the time step has to be much smaller than ℓ . We need

- $\Delta\tau_{\text{opt}} = 5.10^{-2}$ fm for $\sigma = 1$ mb ,

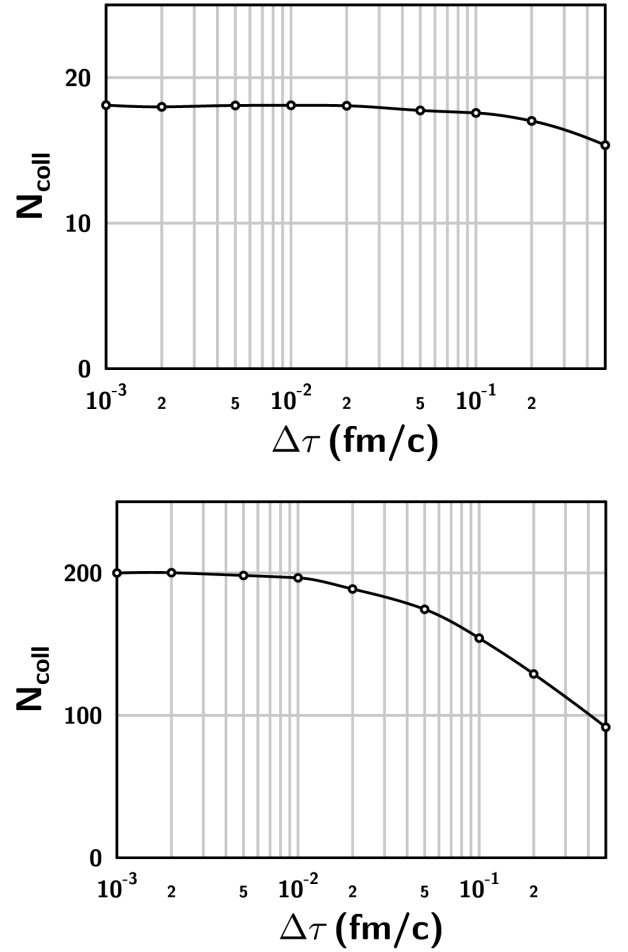


FIG. 17: Total number of collisions for the same initial condition in a box simulation as a function of the time step $\Delta\tau$ for a constant cross section of 1 mb (top) and 5 mb (bottom).

- $\Delta\tau_{\text{opt}} = 10^{-2}$ fm for $\sigma = 5$ mb .

To be on the safe side in our simulations we use

$$\Delta\tau_{\text{opt}} = (1000 \langle v_{\text{rel.}} \rangle \langle \sigma \rangle \langle \rho \rangle)^{-1} \quad (146)$$

with the mean cross section $\langle \sigma \rangle$ calculated from the collisions during the previous time step, the mean relative velocity $\langle v_{\text{rel.}} \rangle$ and the mean scalar density $\langle \rho \rangle$ calculated for each time step.

V. RESULTS

A. Set up of the simulations

The results we present here are obtained for simulations of Au-Au collisions at RHIC energies, $\sqrt{s_{NN}} = 200$ AGeV, or for Pb-Pb collisions at LHC energies, $\sqrt{s_{NN}} = 2760$ AGeV. We use the HPM (see subsection IV A) for the initial condition.

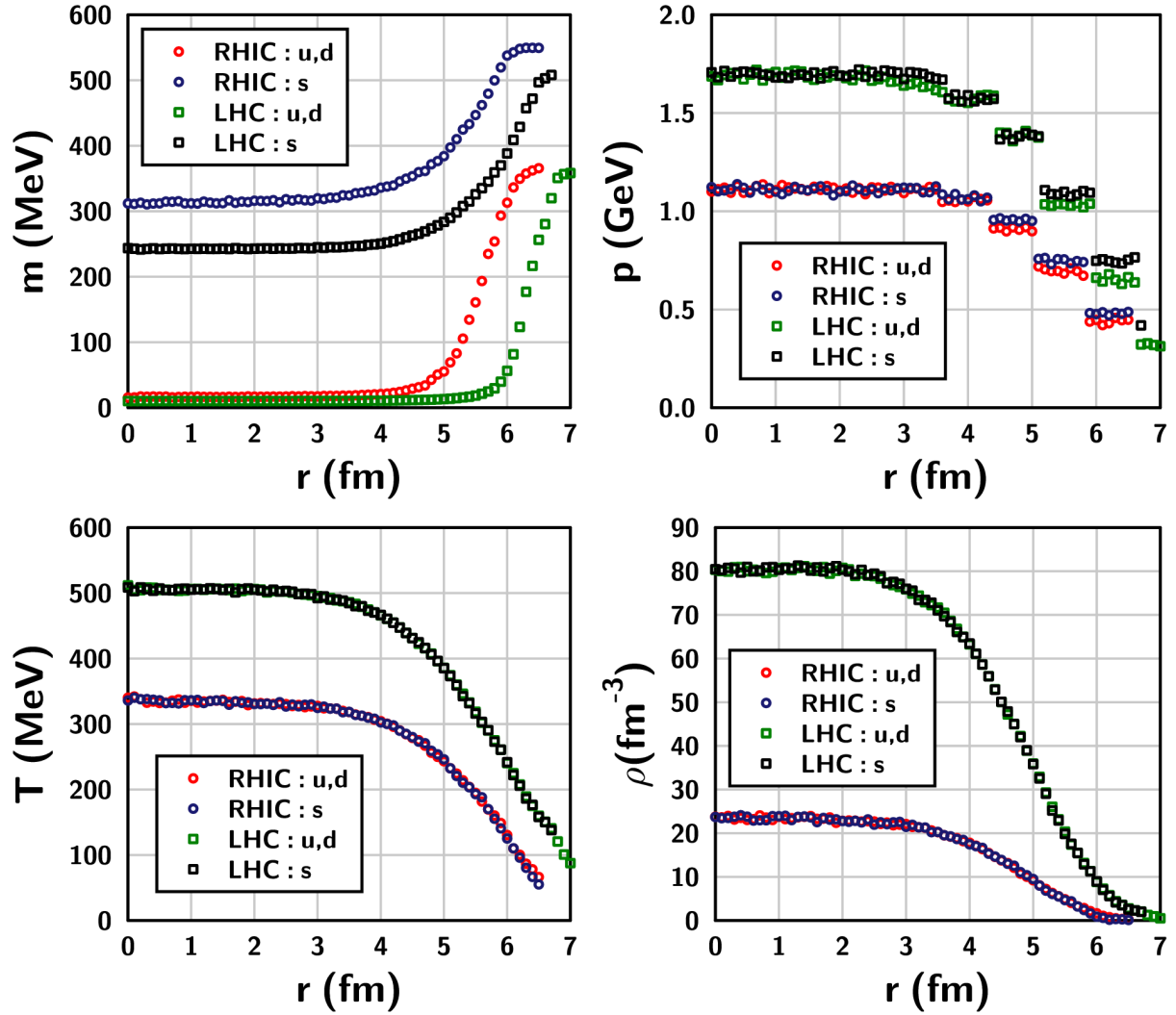


FIG. 18: Distribution of the mass (top left), of the momentum (top right), of the temperatures (bottom left) and of the scalar density (bottom right) for light and strange quarks as a function of the distance r from the centre and for central collisions.

Fig. 18 displays results for central collisions. We show the mass, the momentum, the temperature and density of the light (u , d) and heavy (s) quarks for RHIC and LHC initial conditions as a function of the position of the quarks measured with respect to the centre of the collision. In the centre the quark mass is close to the bare mass. The more the surface is approached, where the density is smaller and the temperature lower, the mass increases and close to the surface we approach the constituent quark mass. The decreasing temperature is also responsible for the decrease of the average momentum. Finally, a smaller temperature yields also a decrease of the density when the surface is approached.

In passing we notice that our smooth initial condition (Fig. 12) is not very realistic if one wants to compare quantitatively our results with experiments. Calculations in models like EPOS [40] show initial energy fluctuations, as seen in Fig. 19. Such fluctuations are visible in the final spectra of the mesons and can therefore not be ne-

glected. We leave calculations with such realistic initial conditions to future investigations.

Fig. 20 shows the number of initial partons and final particles (partons or hadrons) as a function of the impact parameter (the number of partons can increase due to the decay of mesons). The number of particles increases strongly with the centrality of the collisions and therefore also the computing time. The complexity of molecular dynamics calculations manifests itself in the fact that due to the two body potential and due to the collisions the computing time is quadratic in $\mathcal{O}(N^2)$. Adaptive algorithms have been developed which reduces this dependence for large systems to $\mathcal{O}(N \log(N))$ [41] or even to $\mathcal{O}(N)$ (as the program of [42]). Unfortunately our approach does not fulfil the condition for such a simplification. Therefore central collisions are very time consuming and only little statistics has been acquired up to now.

One may use parallelization on supercomputers, or

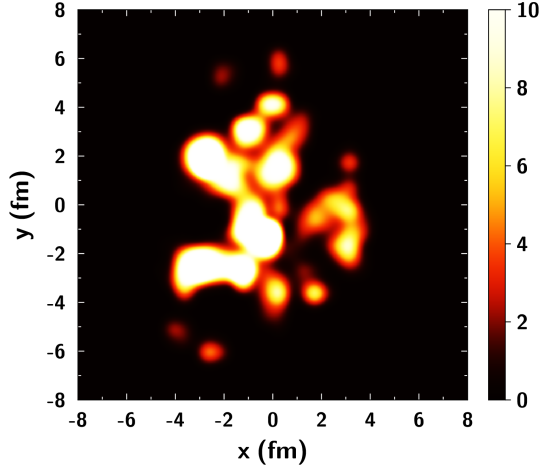


FIG. 19: Energy density distribution (in GeV/fm^3) in the transverse plane x, y for EPOS [43] for a RHIC collision at $b = 6$ fm. Coloured areas are QGP bubbles.

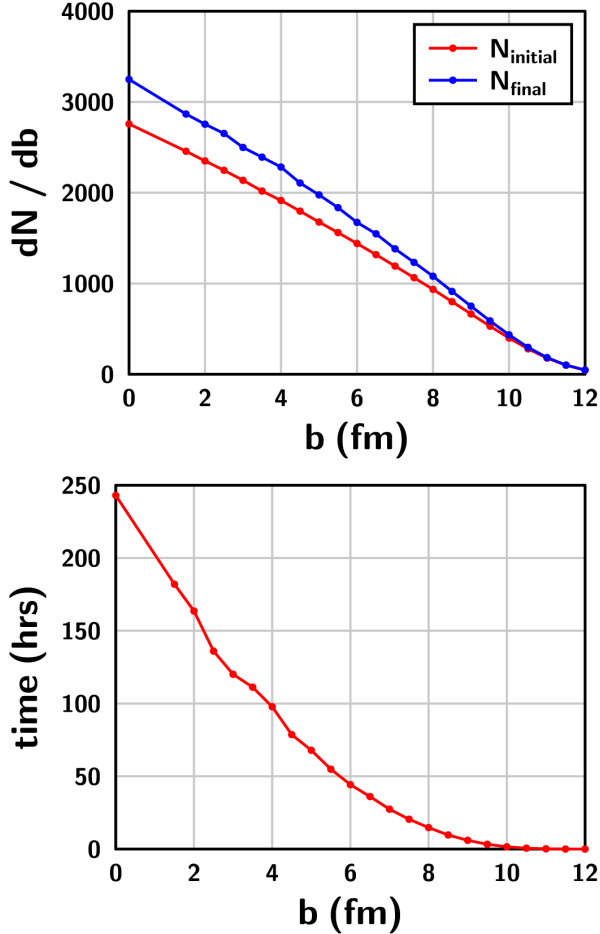


FIG. 20: Number of initial and final particles (top) and computation time per simulation (bottom) as a function of the impact parameter b on a computer with monocore-CPU@3 GHz.

more recently on graphic cards, to make the calculation feasible. In such an approach the calculation is decomposed in small subtasks which can be executed independently. In our approach most of subtasks can be parallelized and therefore the dependence of the calculation time on the particle number can be reduced by a factor

$$R = \frac{1}{(1-s) + \frac{s}{N}}, \quad (147)$$

where N is the number of processors and s the fraction of parallel tasks (in percent). In the ideal case of a code which is to 100% parallel and N is very large, the calculation time is then $\mathcal{O}(N^2) \rightarrow \mathcal{O}(N)$. This parallelization requires the reprogramming of parts of the program and is therefore a project for the future.

B. Check of the algorithm

The most important check for the consistency of the derivation and its numerical realization is the energy conservation. In molecular dynamics calculation it has to be strictly conserved. Fig. 21 displays the variation of the total energy of the system as a function of time for a simulation of a central RHIC collision. Such a simulation contains a couple of thousand partons. We see on the right plot that the energy varies by less than 0.2 %. The small variation of the total energy doesn't come from the solution of the differential equation (Euler or Runge-Kutta), but from the local density jump when a meson decay appears in a "low" density area.

C. First results

In this section we present some preliminary results which we have obtained for RHIC and LHC energies. They show that basic observables are well reproduced in our approach. In Fig. 22 we display the elliptic flow, v_2 , as a function of the impact parameter. These results are compared with the experimental data from the PHOBOS collaboration [44]. We see that the results of our approach agrees quantitatively quite well with the experimental finding. In this plot error bars are not the root mean square, but the variance of mean value after N simulations. This explains the huge error bars for small impact parameters because of the large number of particles and the small number of simulations N .

Fig. 23 displays how the elliptic flow develops as a function of time. On the top we display our results and on the bottom that one of PHSD calculations [45]. By definition there is initially no elliptic flow (assuming thermal equilibrium). In both calculations the flow develops very similarly and both calculations agree also on the final value. In our case, despite of the small cross section of about 1-2 mb, we observe initially many collisions due to the high density. They thermalize the plasma rapidly

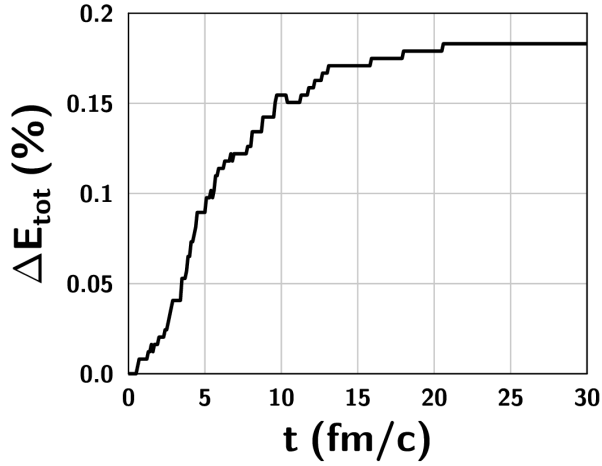


FIG. 21: Variation of the total energy for a central RHIC collision as a function of time.

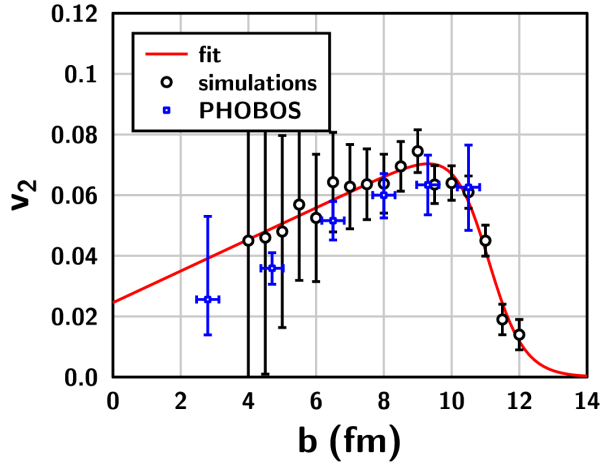


FIG. 22: v_2 as compared to experimental data from the PHOBOS experiment [44] as a function of the impact parameter b .

and lead to an elliptic flow in less than 1 fm/c. The flow is lowered later by the change of the NJL masses.

Experimentally it has been found that the transverse momentum spectra of π and K have a different shape [46]. This can be seen in Fig. 24, bottom, where we compare the experimental data with results from hydrodynamical calculations [47]. On the top we display our results. We observe the same difference of the slopes as seen in experiment which is usually attributed to the hydrodynamical evolution of the system. The lines are there to guide the eyes.

Fig. 25 displays a contour plot of the number of collisions as a function of the distance to the centre of the initial ellipse r and of the time t . On the top we display inelastic collisions on the bottom elastic collisions.

Initially we have a very high density zone where elastic and inelastic collisions take place frequently because the mean free path is small despite of the small cross section.

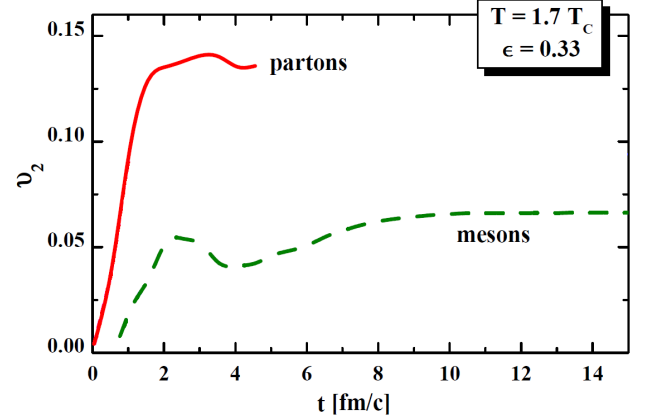
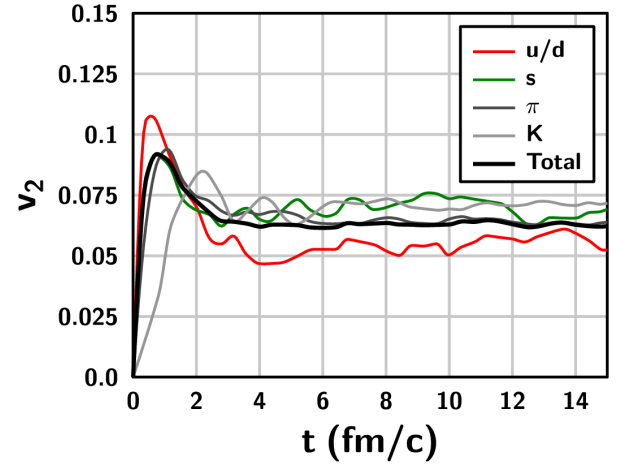


FIG. 23: Time evolution of the elliptic flow v_2 for $b = 6$ fm (top), and the comparison with PHSD calculations for similar initial conditions [45] (bottom).

When the system expands the density becomes lower but the cross section does not increase. Therefore we observe less collisions. When the system approaches the critical temperature the cross sections becomes very large, this compensates by far the decrease of the density and there the collision rate becomes large again for elastic as well as for inelastic collisions. Here the hadrons are created which finally survive.

For the LHC initial condition, Fig. 26, we see the same phenomenon but a longer lifetime of the plasma. In contradistinction to simulation for RHIC energies the corona partons do not hadronize early but the stream of partons from the interior heats up the surface. So the system expands in the quark phase and hadronization takes place only much later over a large space time area.

Fig. 27 shows the distribution of \sqrt{s} and of T at which the final hadrons are produced. We see a broad distribution around the critical temperature and not a single freeze out temperature as assumed in the Cooper-Frye formula [48] which is used to created hadrons in hydrodynamical calculations [47]. The temperature at the K production points is slightly lower than that for the π

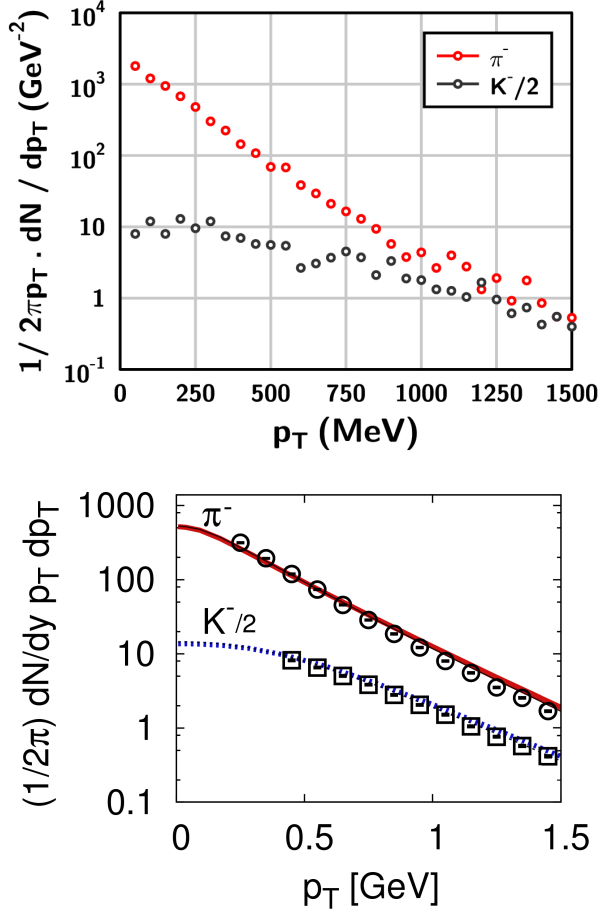


FIG. 24: The $dN/2\pi p_T dp_T$ spectrum for $b = 4$ fm (top), and the results of a hydrodynamical calculation and of the experiment for similar conditions (centrality 0-5%)(bottom) [47].

production points as expected by the NJL cross sections.

Fig. 28 compares the hadronization in our approach (top) with the results of PHSD calculations (bottom) [45]. We observe in both calculations a hadronization time of around 5 fm/c for the RHIC conditions. The difference between the particle number of PHSD and in our model comes from the fact that we have a different initial conditions. Of course the hadronisation is longer for the LHC initial condition (top right) due to the higher density of partons.

VI. SUMMARY

We have presented in this paper a relativistic molecular dynamics approach. We have shown that for a specific choice of the constraints it is possible to find back the *classical* relativistic equations of motion. These constraints give us physical trajectories with causal motion and the conservation of the energy of a strongly interacting system. Using the Nambu-Jona-Lasinio Lagrangian

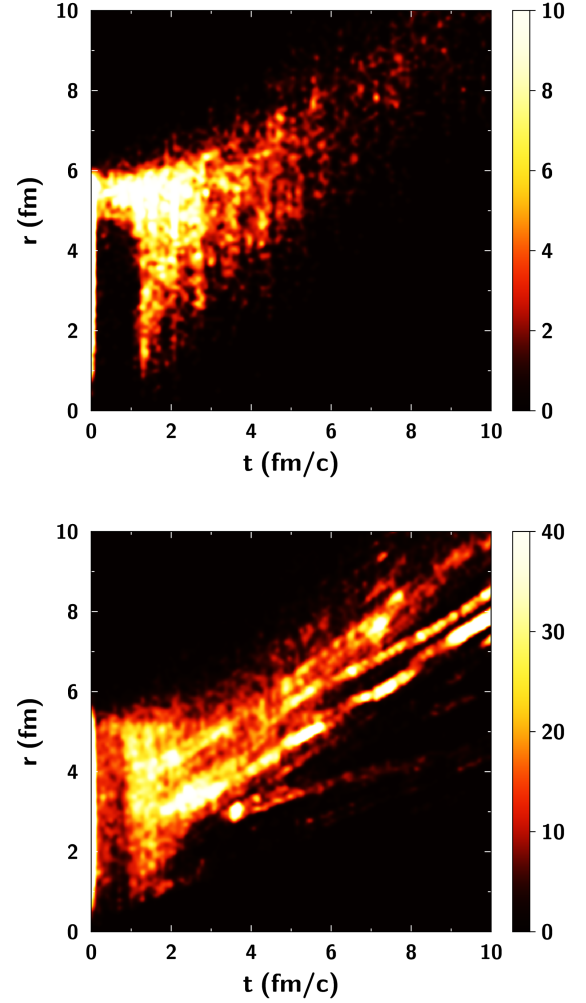


FIG. 25: (t, r) distributions for inelastic (top) and elastic (bottom) collisions at $b = 0$ fm for RHIC conditions.

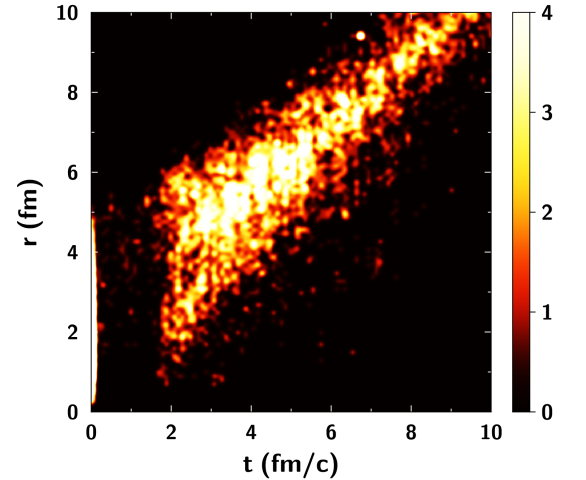


FIG. 26: (t, r) distributions for inelastic collisions at $b = 9$ fm for LHC conditions.

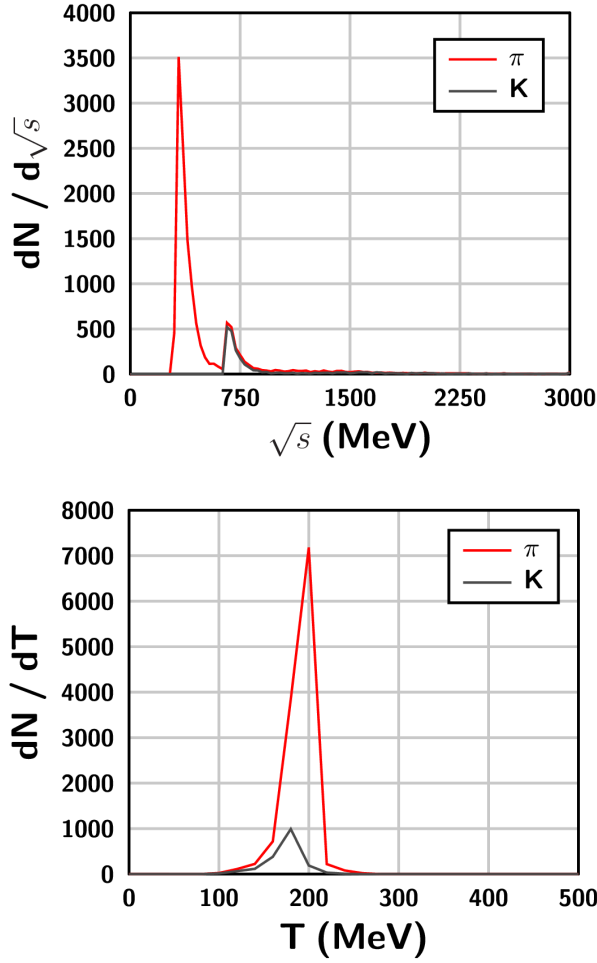


FIG. 27: \sqrt{s} distribution for inelastic collisions (top), and the distribution of the temperature at the production points, T , for pions and kaons (bottom).

to describe the potential interactions and the scattering among the partons we find that it is possible to model the expansion of a quark anti-quark plasma. Close to the cross over the elastic as well as the hadronization cross sections explode. The large hadronization cross section is the reason that the large majority of the quarks form mesons which can finally be observed.

We presented first result which show that a approach which does not enforce local equilibrium, as hydrodynamics, and in which the transition to the hadronic world is not sudden, as in the Cooper Frye approach, used frequently in hydrodynamical calculations, gives qualitative agreement with some key observables. Further studies for a in depth comparison with the existing models will be the subject of a future publication.

The approach is in spirit close to the PHSD approach but differs completely as far as the temperature and density dependence of the mass of the quarks is concerned. Therefore it will be fruitful to compare the observables which are obtained in both approaches for the same initial condition.

VII. ACKNOWLEDGMENT

We thank E. Bratkovskaya and W. Cassing for fruitful discussions and E. Bratkovskaya also for her continuous interest. R. Marty especially thanks the “HIC for FAIR” framework of the “LOEWE” program for the support of this work. The computational resources were provided by the LOEWE-CSC.

-
- [1] T. Hirano, P. Huovinen, and Y. Nara, Phys. Rev. C **84**, 011901 (2011).
 - [2] K. Werner, I. Karpenko, T. Pierog, M. Bleicher, and K. Mikhailov, Phys. Rev. C **82**, 044904 (2010).
 - [3] M. Luzum and P. Romatschke, Phys. Rev. C **78**, 034915 (2008).
 - [4] J. Aichelin and K. Werner, Journal of Physics G: Nuclear and Particle Physics **37**, 094006 (2010).
 - [5] W. Cassing, Eur. Phys. J. ST **168**, 3 (2009).
 - [6] W. Cassing and E. L. Bratkovskaya, Nucl. Phys. A **831**, 215 (2009).
 - [7] E. L. Bratkovskaya, W. Cassing, V. P. Konchakovski, and O. Linnyk, Nucl. Phys. A **856**, 162 (2011).
 - [8] J. Uphoff, O. Fochler, Z. Xu, and C. Greiner, Phys. Rev. C **82**, 044906 (2010).
 - [9] P. Rehberg, L. Bot, and J. Aichelin, Nucl. Phys. A **653**, 415 (1999).
 - [10] S. Klimt, M. F. M. Lutz, U. Vogl, and W. Weise, Nucl. Phys. A **516**, 429 (1990).
 - [11] R. Nebauer and J. Aichelin, Phys. Rev. C **65**, 045204 (2002).
 - [12] C. Ratti, S. Roessner, M. A. Thaler, and W. Weise, Eur. Phys. J. C **49**, 213 (2007).
 - [13] P. Rehberg, S. P. Klevansky, and J. Hufner, Phys. Rev. C **53**, 410 (1996).
 - [14] F. Gastineau, E. Blanquier, and J. Aichelin, Phys. Rev. Lett. **95**, 052001 (2005).
 - [15] H. Sorge, H. Stöcker, and W. Greiner, Annals Phys. **192**, 266 (1989).
 - [16] J. Aichelin, Phys. Rept. **202**, 233 (1991).
 - [17] A. Le Fèvre, J. Aichelin, C. Hartnack, et al., Phys. Rev. C **80**, 044615 (2009).
 - [18] C. Hartnack, H. Oeschler, Y. Leifels, E. L. Bratkovskaya, and J. Aichelin (2012), arXiv:1106.2083v2 [nucl-th].
 - [19] C. Hartnack, H. Oeschler, and J. Aichelin, Phys. Rev. Lett. **96**, 012302 (2006).
 - [20] E. C. G. Sudarshan, N. Mukunda, and J. N. Goldberg, Phys. Rev. D **23**, 2218 (1981).
 - [21] P. A. M. Dirac, Canad. J. math. **2**, 129 (1950).
 - [22] A. Kihlberg, R. Marnelius, and N. Mukunda, Phys. Rev.

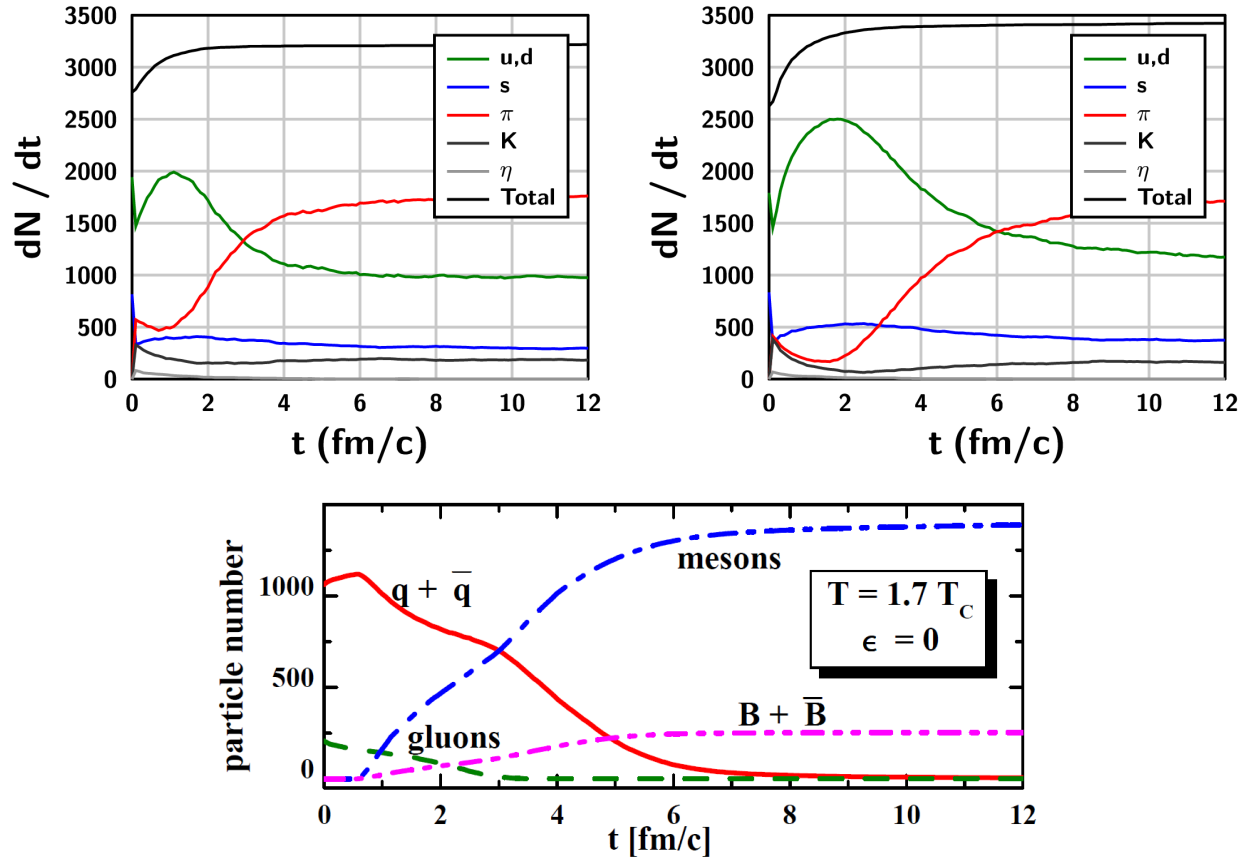


FIG. 28: dN/dt for our simulations at $b = 0$ fm and RHIC conditions (top left) and $b = 9$ and LHC conditions (top right), and for PHSD for $b = 0$ fm and RHIC conditions (bottom) [45].

- D **23**, 2201 (1981).
- [23] F. Rohrlich, Ann. Phys. **117**, 292 (1979).
 - [24] J. Samuel, Phys. Rev. D **26**, 3475 (1982).
 - [25] N. Mukunda and E. C. G. Sudarshan, Phys. Rev. D **23**, 2210 (1981).
 - [26] I. T. Todorov, Lecture Notes in Physics **162**, 213 (1982).
 - [27] T. Maruyama, S. W. Huang, et al., Nucl. Phys. A **534**, 720 (1991).
 - [28] S. A. Bass, M. Belkacem, et al., Prog. Part. Nucl. Phys. **41**, 255 (1998).
 - [29] S. P. Klevansky, Rev. Mod. Phys. **64**, 649 (1992).
 - [30] D. Ebert, H. Reinhardt, and M. Volkov, Prog.Part.Nucl.Phys. **33**, 1 (1994).
 - [31] F. Gastineau and J. Aichelin, J. Phys. G **28**, 2017 (2002).
 - [32] F. Gastineau, Ph.D. thesis, Universit de Nantes (2002).
 - [33] M. Lutz, S. Klimt, and W. Weise, Nucl. Phys. A **542**, 521 (1992).
 - [34] M. Buballa, Phys. Rept. **407**, 205 (2005).
 - [35] E. Quack and S. P. Klevansky, Phys. Rev. C **49**, 3283 (1994).
 - [36] P. Rehberg, S. P. Klevansky, and J. Hufner, Nucl. Phys. A **608**, 356 (1996).
 - [37] J. Hufner, S. Klevansky, E. Quack, and P. Zhuang, Phys. Lett. B **337**, 30 (1994).
 - [38] M. Thomère, Ph.D. thesis, Université de Nantes (2009).
 - [39] R. Nebauer, Ph.D. thesis, Université de Nantes (2000).
 - [40] H. J. Drescher, M. Hladik, S. Ostapchenko, T. Pierog, and K. Werner, Phys. Rept. **350**, 93 (2001).
 - [41] R. Yokota and L. A. Barba (2011), arXiv:1108.5815v2 [cs.NA].
 - [42] M. N. Bannerman, R. Sargant, and L. Lue (2010), arXiv:1004.3501v2 [physics.comp-ph].
 - [43] K. Werner, *Hydrodynamic evolution with flux tube (EPOS) initial conditions* (2009), [WWND meeting](#).
 - [44] B. Alver et al., Phys. Rev. Lett. **98**, 242302 (2007).
 - [45] W. Cassing and E. L. Bratkovskaya, Phys. Rev. C **78**, 034919 (2008).
 - [46] E. Schnedermann, J. Sollfrank, and U. Heinz, Phys. Rev. C **48**, 2462 (1993).
 - [47] B. Schenke, S. Jeon, and C. Gale, Phys. Rev. C **82**, 014903 (2010).
 - [48] F. Cooper and G. Frye, Phys. Rev. D **10**, 186 (1974).

Appendix

1. Relativistic calculations

a. Derivatives of transverse distances

The calculation of the derivatives for transverse distances can be done rigorously

$$\begin{aligned}
\frac{\partial q_{Tij}^2}{\partial q_{k\nu}} &= 2q_{Tij\mu} \frac{\partial q_{Tij}^\mu}{\partial q_{k\nu}} \\
&= 2q_{Tij\mu} \frac{\partial}{\partial q_{k\nu}} (q_{ij}^\mu - (q_{ij\sigma} u_{ij}^\sigma) u_{ij}^\mu) \\
&= 2q_{Tij\mu} \left[(\delta_{ik} - \delta_{jk}) \eta^{\mu\nu} \right. \\
&\quad \left. - \frac{\partial (q_{ij\sigma} u_{ij}^\sigma)}{\partial q_{k\nu}} u_{ij}^\mu - (q_{ij\sigma} u_{ij}^\sigma) \frac{\partial u_{ij}^\mu}{\partial q_{k\nu}} \right] \quad (148)
\end{aligned}$$

$$\frac{\partial q_{Tij}^2}{\partial q_{k\nu}} = 2q_{Tij}^\nu (\delta_{ik} - \delta_{jk}).$$

$$\begin{aligned}
\frac{\partial q_{Tij}^2}{\partial p_{k\nu}} &= 2q_{Tij\mu} \frac{\partial q_{Tij}^\mu}{\partial p_{k\nu}} \\
&= 2q_{Tij\mu} \frac{\partial}{\partial p_{k\nu}} (q_{ij}^\mu - (q_{ij\sigma} u_{ij}^\sigma) u_{ij}^\mu) \\
&= 2q_{Tij\mu} \left[0 \right. \\
&\quad \left. - \frac{\partial (q_{ij\sigma} u_{ij}^\sigma)}{\partial p_{k\nu}} u_{ij}^\mu - (q_{ij\sigma} u_{ij}^\sigma) \frac{\partial u_{ij}^\mu}{\partial p_{k\nu}} \right] \quad (149) \\
\frac{\partial q_{Tij}^2}{\partial p_{k\nu}} &= -2q_{Tij}^\nu (\delta_{ik} + \delta_{jk}) \frac{(q_{ij\sigma} u_{ij}^\sigma)}{\sqrt{p_{ij}^2}}.
\end{aligned}$$

and the same kind of derivatives can be found for q'_T :

$$\begin{aligned}
\frac{\partial q_{Tij}'^2}{\partial q_{k\nu}} &= 2q_{Tij'\mu} \frac{\partial q_{Tij}'^\mu}{\partial q_{k\nu}} \\
&= 2q_{Tij'\mu} \frac{\partial}{\partial q_{k\nu}} (q_{ij}^\mu - (q_{ij\sigma} U^\sigma) U^\mu) \\
&= 2q_{Tij'\mu} \left[(\delta_{ik} - \delta_{jk}) \eta^{\mu\nu} \right. \\
&\quad \left. - \frac{\partial (q_{ij\sigma} U^\sigma)}{\partial q_{k\nu}} U^\mu - (q_{ij\sigma} U^\sigma) \frac{\partial U^\mu}{\partial q_{k\nu}} \right] \quad (150) \\
\frac{\partial q_{Tij}'^2}{\partial q_{k\nu}} &= 2q_{Tij'}^\nu (\delta_{ik} - \delta_{jk}).
\end{aligned}$$

$$\begin{aligned}
\frac{\partial q_{Tij}'^2}{\partial p_{k\nu}} &= 2q_{Tij'\mu} \frac{\partial q_{Tij}'^\mu}{\partial p_{k\nu}} \\
&= 2q_{Tij'\mu} \frac{\partial}{\partial p_{k\nu}} (q_{ij}^\mu - (q_{ij\sigma} U^\sigma) U^\mu) \\
&= 2q_{Tij'\mu} \left[0 \right. \\
&\quad \left. - \frac{\partial (q_{ij\sigma} U^\sigma)}{\partial p_{k\nu}} U^\mu - (q_{ij\sigma} U^\sigma) \frac{\partial U^\mu}{\partial p_{k\nu}} \right] \quad (151) \\
\frac{\partial q_{Tij}'^2}{\partial p_{k\nu}} &= -2q_{Tij'}^\nu \frac{(q_{ij\sigma} U^\sigma)}{\sqrt{P^2}} \stackrel{\text{lab}}{=} 0.
\end{aligned}$$

b. Matrix of constraints

We present the full calculation of the matrix of constraints and the full expression of the equations of motion for the case in which the KT [26] condition is not fulfilled. We start with the calculation of the derivative of the first constraints

$$\begin{aligned}
\frac{\partial K_i}{\partial q_k^\mu} &= \frac{\partial V_i}{\partial q_k^\mu}, \\
\frac{\partial K_i}{\partial p_k^\mu} &= 2p_{i\mu} \delta_{ik} + \frac{\partial V_i}{\partial p_k^\mu}. \quad (152)
\end{aligned}$$

Then for time constraint

$$\begin{aligned}
\frac{\partial \chi_i}{\partial q_k^\mu} &= \sum_{j \neq i} (\delta_{ik} - \delta_{jk}) \frac{U_\mu}{N}, \\
\frac{\partial \chi_i}{\partial p_k^\mu} &= \frac{1}{N\sqrt{P^2}} \sum_{j \neq i} q_{ij}^\nu \Omega_{\nu\mu}. \quad (153)
\end{aligned}$$

and

$$\begin{aligned}
\frac{\partial \chi_N}{\partial q_k^\mu} &= \frac{U_\mu}{N}, \\
\frac{\partial \chi_N}{\partial p_k^\mu} &= \frac{1}{N\sqrt{P^2}} \sum_j q_j^\nu \Omega_{\nu\mu} \quad (154)
\end{aligned}$$

We notice that except $\partial\chi_i/\partial q_k^\mu$, the derivatives of χ don't depend on k . For the full matrix of constraints we find

$$\begin{aligned}
\{K_i, \chi_j\} &= \sum_k \left[\left(\frac{\partial V_i}{\partial q_k^\mu} \right) \left(\frac{1}{N\sqrt{P^2}} \sum_{l \neq j} q'_{Tjl\mu} \right) \right. \\
&\quad \left. - \left(2p_i^\mu \delta_{ik} + \frac{\partial V_i}{\partial p_k^\mu} \right) \left(\sum_{l \neq j} (\delta_{jk} - \delta_{lk}) \frac{U_\mu}{N} \right) \right] \\
&= \underbrace{\left(\sum_k \frac{\partial V_i}{\partial q_k^\mu} \right)}_{=0} \left(\frac{1}{N\sqrt{P^2}} \sum_{l \neq j} q'_{Tjl\mu} \right) \\
&\quad - \left(N \frac{\partial V_i}{\partial p_j^\mu} - \sum_l \frac{\partial V_i}{\partial p_l^\mu} \right) \frac{U_\mu}{N} \\
&\quad - \left(\frac{2p_i^\mu U_\mu}{N} \sum_{l \neq j} (\delta_{ji} - \delta_{li}) \right) \\
\{K_i, \chi_j\} &= - \left(N \frac{\partial V_i}{\partial p_j^\mu} - \sum_l \frac{\partial V_i}{\partial p_l^\mu} \right) \frac{U_\mu}{N} \\
&\quad - \left(\frac{2p_i^\mu U_\mu}{N} \sum_{l \neq j} (\delta_{ji} - \delta_{li}) \right).
\end{aligned} \tag{155}$$

$$\begin{aligned}
\{K_i, \chi_N\} &= \sum_k \left[\left(\frac{\partial V_i}{\partial q_k^\mu} \right) \left(\frac{1}{N\sqrt{P^2}} \sum_l q'_{Tl\mu} \right) \right. \\
&\quad \left. - \left(2p_i^\mu \delta_{ik} + \frac{\partial V_i}{\partial p_k^\mu} \right) \left(\frac{U_\mu}{N} \right) \right] \\
&= \underbrace{\left(\sum_k \frac{\partial V_i}{\partial q_k^\mu} \right)}_{=0} \left(\frac{1}{N\sqrt{P^2}} \sum_l q'_{Tl\mu} \right) \\
&\quad - \left(\sum_k \frac{\partial V_i}{\partial p_k^\mu} \right) \frac{U_\mu}{N} - \left(\frac{2p_i^\mu U_\mu}{N} \right) \\
\{K_i, \chi_N\} &= - \left(\sum_k \frac{\partial V_i}{\partial p_k^\mu} \right) \frac{U_\mu}{N} \\
&\quad - \left(\frac{2p_i^\mu U_\mu}{N} \right).
\end{aligned} \tag{156}$$

Using eq. (82), we can write :

$$\begin{aligned}
\{\chi_i, \chi_j\} &= \sum_k \left[\left(\sum_{l \neq i} (\delta_{ik} - \delta_{lk}) \frac{U^\mu}{N} \frac{1}{N\sqrt{P^2}} \sum_{m \neq j} q'_{Tjm\mu} \right) \right. \\
&\quad \left. - \frac{1}{N\sqrt{P^2}} \sum_{l \neq i} q'_{Til} \sum_{l \neq j} (\delta_{jk} - \delta_{lk}) \frac{U_\mu}{N} \right] = 0.
\end{aligned} \tag{157}$$

$$\begin{aligned}
\{\chi_i, \chi_N\} &= \sum_k \left[\left(\sum_{l \neq i} (\delta_{ik} - \delta_{lk}) \frac{U^\mu}{N} \frac{1}{N\sqrt{P^2}} \sum_m q'_{Tm\mu} \right) \right. \\
&\quad \left. - \frac{1}{N\sqrt{P^2}} \sum_{l \neq i} q'_{Til} \frac{U_\mu}{N} \right] = 0.
\end{aligned} \tag{158}$$

$$\{\chi_N, \chi_N\} = 0. \tag{159}$$

We can summarize these results presenting the complete matrix of constraint :

$$C_{ij}^{-1} = \{\phi_i, \phi_j\} = \begin{pmatrix} \{K_i, K_j\} & \{K_i, \chi_j\} \\ \{\chi_i, K_j\} & \{\chi_i, \chi_j\} \end{pmatrix} \tag{160}$$

with

$$\begin{aligned}
A_{ij}^{-1} &= \{K_i, K_j\} \neq 0 \\
B_{ij}^{-1} &= \{\chi_i, \chi_j\} = 0 \\
S_{ij}^{-1} &= \{\chi_i, K_j\} \neq 0
\end{aligned} \tag{161}$$

That gives us the following relativistic factor :

$$\lambda_k = C_{2Nk} \quad 1 < k < 2N. \tag{162}$$

The final expression for the equations of motion is :

$$\begin{aligned}
\frac{dq_i^\mu}{d\tau} &= 2\lambda_i p_i^\mu + \sum_{k=1}^N \lambda_k \frac{\partial V_k(q'_T)}{\partial p_{i\mu}} + \frac{1}{N\sqrt{P^2}} \\
&\quad \left[\left(\sum_{j \neq i} q'_{Tij\mu} \right) \sum_{k=N+1}^{2N-1} \lambda_k + \left(\sum_j q'_{Tj\mu} \right) \lambda_N \right] \\
\frac{dp_i^\mu}{d\tau} &= - \sum_{k=1}^N \lambda_k \frac{\partial V_k(q'_T)}{\partial q_{i\mu}} - \frac{U_\mu}{N} \\
&\quad \left[\sum_{k=N+1}^{2N-1} \lambda_k \left(\sum_{j \neq i} (\delta_{ik} - \delta_{jk}) \right) + \lambda_N \right].
\end{aligned} \tag{163}$$

We can write these equations in a simplified form using q'_T and the global reference frame ($U^\mu = (1, 0, 0, 0)$). Please notice that we only use the 3-vector part of these equations :

$$\begin{aligned}
\frac{dq_i^\mu}{d\tau} &= \frac{p_i^\mu}{E_i} + \frac{1}{N\sqrt{P^2}} \\
&\quad \left[\left(\sum_{j \neq i} q'_{Tij\mu} \right) \sum_{k=N+1}^{2N-1} \lambda_k + \left(\sum_j q'_{Tj\mu} \right) \lambda_N \right] \\
\frac{dp_i^\mu}{d\tau} &= - \sum_{k=1}^N \frac{1}{2E_k} \frac{\partial V_k}{\partial q_{i\mu}}.
\end{aligned} \tag{164}$$

The second term of $dq_i^\mu/d\tau$ is embarrassing. For $N = 2$ particles this term is vanishing. Unfortunately for a large number of particles ($2 < N$) it does not disappear. To avoid this the KT condition must be fulfilled.

2. Thermodynamical densities

Eq. (138) can be calculated analytically for $\mu \rightarrow 0$ and $m \ll T$ (including a factor 2 in g) :

$$\begin{aligned}\rho_F &= \frac{4\pi}{(2\pi)^3(\hbar c)^3} g \int_0^\infty (f^+ + f^-) p^2 dp \\ &= \frac{4\pi}{(2\pi)^3(\hbar c)^3} g m^2 T \ell K_2\left(\frac{m}{T}\right) \\ &= \frac{4\pi}{(2\pi)^3(\hbar c)^3} g m^2 T \ell \frac{\Gamma(2)}{2} \left(\frac{2}{m/T}\right)^2 \\ \rho_F &= \frac{\ell g}{\pi^2} \left(\frac{T}{\hbar c}\right)^3.\end{aligned}\quad (165)$$

Then we find :

$$T_i = (\hbar c) \left(\frac{\pi^2}{\ell g}\right)^{1/3} \rho_F^{1/3}. \quad (166)$$

For the baryonic density, eq. (139), we have :

$$\begin{aligned}\rho_B &= \frac{4\pi}{(2\pi)^3(\hbar c)^3} g \int_0^\infty (f^+ - f^-) p^2 dp \\ &= \frac{4\pi}{(2\pi)^3(\hbar c)^3} g \frac{\pi^2}{3} T^3 \left(\frac{\mu}{T} + \left(\frac{\mu}{T}\right)^3 \frac{1}{\pi^2}\right) \\ &= \frac{4\pi}{(2\pi)^3(\hbar c)^3} g \frac{\pi^2}{3} \left(\underbrace{T^2 \mu}_{\text{Low Order}} + \frac{\mu^3}{\pi^2}\right) \\ \rho_B &\approx \frac{g}{6\pi^2} \left(\frac{\mu}{\hbar c}\right)^3.\end{aligned}\quad (167)$$

and finally

$$\mu_i = (\hbar c) \left(\frac{6\pi^2}{g}\right)^{1/3} \rho_B^{1/3}. \quad (168)$$

The degeneracy factor for the spin, the parity, the color and the flavour is $g = 2 \times 2 \times 3 \times 3 = 36$.

3. Derivation of potential

The forces coming from the derivative of the potential are :

$$\begin{aligned}\frac{\partial V_i}{\partial q_{k\nu}} &= \frac{\partial m_i^2}{\partial q_{k\nu}} = 2m_i \frac{\partial m_i}{\partial q_{k\nu}} = 2m_i \frac{\partial m_i}{\partial T_i} \frac{\partial T_i}{\partial q_{k\nu}}, \\ \frac{\partial V_i}{\partial p_{k\nu}} &= \frac{\partial m_i^2}{\partial p_{k\nu}} = 2m_i \frac{\partial m_i}{\partial p_{k\nu}} = 2m_i \frac{\partial m_i}{\partial T_i} \frac{\partial T_i}{\partial p_{k\nu}}.\end{aligned}\quad (169)$$

The local temperature is defined as :

$$T_i = (\hbar c) \left(\frac{\pi^2}{\ell g}\right)^{1/3} \rho_F^{1/3} = \Pi \left(\sum_{l \neq i} R_{il}\right)^{1/3} \quad (170)$$

with $R_{ij} = \exp(q_{Tij}'^2/L^2)$ and

$$\Pi = (\hbar c) \left(\frac{\pi^2}{\ell g}\right)^{1/3} \simeq 190 \text{ MeV}. \quad (171)$$

L is a weighting factor. Its derivatives are :

$$\begin{aligned}\frac{\partial T_i}{\partial q_{k\nu}} &= \Pi \frac{1}{3} \frac{1}{\left(\sum_{l \neq i} R_{il}\right)^{2/3}} \sum_{l \neq i} R_{il} \frac{1}{L^2} \frac{\partial q_T(')_{ij}^2}{\partial q_{k\nu}}, \\ \frac{\partial T_i}{\partial p_{k\nu}} &= \Pi \frac{1}{3} \frac{1}{\left(\sum_{l \neq i} R_{il}\right)^{2/3}} \sum_{l \neq i} R_{il} \frac{1}{L^2} \frac{\partial q_T(')_{ij}^2}{\partial p_{k\nu}},\end{aligned}\quad (172)$$

which can be rewritten :

$$\begin{aligned}\frac{\partial T_i}{\partial q_{k\nu}} &= \frac{2\Pi^3}{3L^2 T_i^2} \sum_{l \neq i} R_{il} q_{Til}'^\nu (\delta_{ik} - \delta_{lk}), \\ \frac{\partial T_i}{\partial p_{k\nu}} &= -\frac{2\Pi^3}{3L^2 T_i^2} \sum_{l \neq i} R_{il} q_{Til}'^\nu \frac{(q_{il\sigma} U^\sigma)}{\sqrt{P^2}} \stackrel{\text{lab}}{=} 0.\end{aligned}\quad (173)$$